

# A MULTISCALE FINITE ELEMENT METHOD FOR OSCILLATING NEUMANN PROBLEM ON ROUGH DOMAIN

PINGBING MING \* AND XIANMIN XU †

**Abstract.** We develop a new multiscale finite element method for Laplace equation with oscillating Neumann boundary conditions on rough boundaries. The key point is the introduction of a new boundary condition that incorporates both the microscopically geometrical and physical information of the rough boundary. Our approach applies to problems posed on domain with rough boundary as well as oscillating boundary conditions. We prove the method has linear convergence rate in the energy norm with a weak resonance term for periodic roughness. Numerical results are reported for both periodic and nonperiodic roughness.

**Key words.** Multiscale finite element method; Rough boundary; Homogenization

**AMS subject classifications.** 65N30; 74Q05.

**1. Introduction.** Many problems in nature and industry applications are described by partial differential equations in domain with multiscale boundary [10, 27]. Some of them even have oscillatory Neumann or Robin boundary conditions on the multiscale boundary [20, 44]. Theoretical study for problems with rough boundary and oscillating boundary data mainly concerns the effective boundary conditions, which may be traced back to [28]. There are extensive work thereafter devoted to various topics in this field, including Poisson problem, eigenvalue problems, and Navier-Stokes equations with different types of boundary conditions; see [4, 9, 19, 29, 35, 36, 37, 39] and the references therein.

Compared to the extensive theoretical study, numerical methods for the rough boundary problem have been less developed, while many numerical methods have been devoted to solve elliptic problems with rough coefficients [6, 7, 8, 5, 26, 24, 25, 13, 14, 40]. We refer to [12, Chapter 8] and [16] for a review on this active field. Only recently, a multiscale finite element method (MsFEM) was introduced to solve Laplace equation with homogeneous Dirichlet boundary value on rough domain [30]. The multiscale basis functions are constructed for the elements near the rough boundary by solving a cell problem with the homogeneous Dirichlet condition on the rough edge and with linear nodal basis function as boundary condition on other edges, just as the

---

\*LSEC, Institute of Computational Mathematics and Scientific/Engineering Computing, AMSS, Chinese Academy of Sciences, No. 55, Zhong-Guan-Cun East Road, Beijing 100190, China. (mpb@lsec.cc.ac.cn) The work of Ming was partially supported by the National Natural Science Foundation of China for Distinguished Young Scholars 11425106, and National Natural Science Foundation of China grants 91230203, and by the funds from Creative Research Groups of China through grant 11021101, and by the support of CAS NCMIS.

†LSEC, Institute of Computational Mathematics and Scientific/Engineering Computing, NCMIS, AMSS, Chinese Academy of Sciences, No. 55, Zhong-Guan-Cun East Road, Beijing 100190, China. (xmxu@lsec.cc.ac.cn) X. Xu acknowledges the financial support by SRF for ROCS, SEM and by NSFC grant 11571354.

standard MsFEM [24]. However, this approach cannot be applied either to problems with non-Dirichlet boundary conditions over rough boundary, or to problems with inhomogeneous Dirichlet boundary value over the rough boundary. Therefore, one of our motivations is to develop a multiscale method for problem with oscillating boundary condition given on the rough boundary.

We introduce a new multiscale finite element method for Laplace equation with oscillating boundary flux on the rough boundary. A Neumann boundary condition that depends on the magnitude of the flux oscillation has to be imposed on the local cell problem posed on elements with rough edge. When the flux oscillation is of the same order of the roughness parameter, the boundary condition contains only the microscopical geometry of the rough boundary. Otherwise, one has to incorporate both the microscopical geometry of the rough boundary and the flux oscillation into the boundary condition. Such multiscale basis function coincides with the linear nodal basis functions for elements without a rough edge. This method is  $H^1$ -conforming, with degrees of freedom at the mesh nodes and the basis functions are solved over the elements near the rough boundary and can be computed off line. For periodic roughness, we prove that our method has optimal convergence rate in the energy norm besides a weak resonance term. The method also applies to problems with non-periodic roughness as demonstrated by the numerical experiments. The proof is based on certain homogenization results for Neumann rough boundary value problems, which refine the corresponding results in [19] by clarifying the dependence of the error bounds on the domain size. Our convergence results require that the right-hand side function  $f \in H^1$ . However, numerical experiments show that the optimal convergence order is retained for even rougher  $L^2$  right-hand side function.

The novelty of the proposed method is that both the rough boundary and the oscillating flux are considered and no structure is assumed for the oscillations. The method can be naturally generalized to the inhomogeneous Dirichlet boundary value problem over rough domain. It is also possible to combine the proposed method with the standard MsFEM to deal with the problems with oscillatory coefficients and oscillatory boundary data.

The so-called composite finite elements has been successfully applied to solve boundary value problems over complicated domain [21, 22, 41]. The basic idea of this method is to incorporate the geometrical complexity of the domain into the basis function, while there is no local cell problems. Optimal convergence rate has been achieved, which is independent of the geometrical structure of the domain [21, 38, 42]. In particular, homogeneous Neumann boundary value problems have been studied in [21] and [38]. In contrast to composite finite elements, the multiscale basis function is constructed by solving local problem that contains both the geometry complexity and the oscillation of the boundary flux.

A multiscale method has been developed for elliptic equation with homogeneous boundary condition on complicated domains very recently in [18]. The method is

based on the localized orthogonal decomposition (LOD) technique developed in [31, 17, 32, 23, 33]. The method is quite general and has optimal convergence order. The difference between LOD method and the proposed method is the way in dealing with the multiscale basis function near the rough boundary. In the LOD method, cell problems are solved in several layers of elements near the boundary. In our method, the multiscale basis functions are solved only in cells with rough boundary. When the underlying scales of the problem are well-separated, MsFEM would be less expensive. Furthermore, we study the inhomogeneous oscillating flux on the boundary while only homogeneous boundary conditions have been treated in [18]. In addition, we note that the heterogeneous multiscale method and MsFEM have been employed to solve partial differential equations on a rough surface in [1] and [15], respectively, however, the authors have not dealt with the problems studied in this paper.

Finally, the problem with complicated domain can be discretized by adaptive finite element method [43]. However, the mesh size of the adaptive method must be much smaller than the characteristic length scale of the roughness for the sake of resolution, which would result in a linear algebraic system with large condition number. In contrast to the adaptive method, the condition number of the resulting linear system of the proposed method is proportional to  $\mathcal{O}(h^{-2})$  as demonstrated in the numerical experiment, while the coarse grid size  $h$  is not necessarily smaller than the roughness length scale.

The structure of the paper is as follows. In Section 2, we describe the model problem and introduce the multiscale finite element method. In Section 3, we revisit the homogenization results for a Poisson equation with an oscillatory Neumann boundary condition over rough domain. In Section 4, we estimate the convergence rate in energy norm of the proposed method. Numerical examples are illustrated in the last section.

**2. The Model Problem and Multiscale Finite Element Method.** Let  $\Omega_\varepsilon \subset \mathbb{R}^2$  be a bounded domain with boundary  $\partial\Omega_\varepsilon$ , a part of which is rough and denoted as  $\Gamma_\varepsilon$ , where  $\varepsilon$  is a small parameter that characterizes the roughness of  $\Gamma_\varepsilon$ . We consider a model problem with Neumann boundary conditions on  $\Gamma_\varepsilon$ : Given the source term  $f$  and the flux  $g_\varepsilon$  that is oscillatory, we find  $u^\varepsilon$  satisfying

$$\begin{cases} -\Delta u^\varepsilon = f(x), & \text{in } \Omega_\varepsilon, \\ u^\varepsilon = 0, & \text{on } \Gamma_D, \\ \frac{\partial u^\varepsilon}{\partial n} = g_\varepsilon(x), & \text{on } \Gamma_\varepsilon, \end{cases} \quad (2.1)$$

where  $\Gamma_D = \partial\Omega_\varepsilon \setminus \Gamma_\varepsilon$ .

For any measurable subset  $D$  of  $\Omega_\varepsilon$ , we define

$$V(D) = \{ v \in H^1(D) \mid v|_{\partial D \setminus \Gamma_\varepsilon} = 0 \}.$$

Here  $H^1(D)$  is the standard Sobolev space, and the notations and definitions for

Sobolev spaces can be found in [2]. To clarify the dependence of the roughness parameter  $\varepsilon$ , we denote  $u^\varepsilon$  the solution of Problem (2.1), whose weak form is: Find  $u^\varepsilon \in V(\Omega_\varepsilon)$  such that

$$a(u^\varepsilon, v) = (f, v) + (g_\varepsilon, v)_{\Gamma_\varepsilon} \quad \text{for all } v \in V(\Omega_\varepsilon), \quad (2.2)$$

where

$$a(u^\varepsilon, v) := \int_{\Omega_\varepsilon} \nabla u^\varepsilon \cdot \nabla v \, dx, \quad (f, v) := \int_{\Omega_\varepsilon} f v \, dx, \quad (g_\varepsilon, v)_{\Gamma_\varepsilon} := \int_{\Gamma_\varepsilon} g_\varepsilon v \, ds.$$

We triangulate  $\Omega_\varepsilon$  by a shape regular mesh  $\mathcal{T}_h$  in the sense of [11], with element  $\tau \in \mathcal{T}_h$  be either a triangle or a quadrilateral, where  $h = \max_{\tau \in \mathcal{T}_h} h_\tau$  with  $h_\tau$  the diameter of  $\tau$ , and  $\mathcal{S}(\tau)$  is a suitable index set for nodes in  $\tau$ . We assume that an element near  $\Gamma_\varepsilon$  has at most one rough edge on the rough boundary and denote such elements by  $\tau_\varepsilon$ ; see Fig. 2.1. For triangular mesh, there are elements that may have only one node on the rough boundary. In Section 5, we shall give more details on the triangulation.

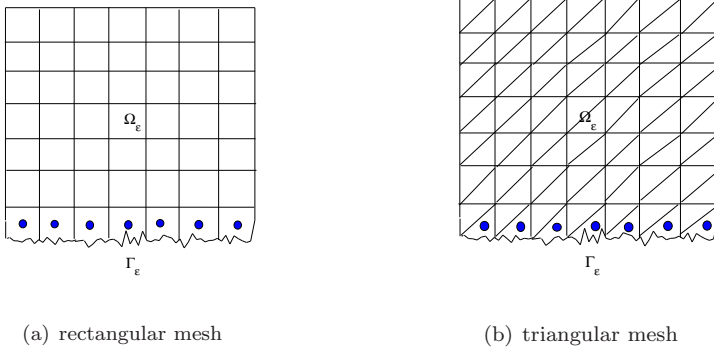


FIG. 2.1. Examples for the triangulation of the domain  $\Omega_\varepsilon$ .

For any measurable subset  $D$  of  $\Omega_\varepsilon$ , we define a localized version of  $a$  as

$$a_D(v, w) := \int_D \nabla v \cdot \nabla w \, dx \quad v, w \in H^1(D).$$

For each  $p \in \mathcal{S}(\tau)$  we construct nodal basis functions  $\Phi_p^{\text{MS}}$ , whose restriction to each element  $\tau$  is denoted by  $\Phi_{p,\tau}^{\text{MS}}$ , which satisfies

$$a_\tau(\Phi_{p,\tau}^{\text{MS}}, v) = (\theta_{p,\tau}, v)_{\partial\tau \cap \Gamma_\varepsilon} \quad \text{for all } v \in V(\tau), \quad (2.3)$$

and  $\Phi_p^{\text{MS}}$  is supplemented with the boundary condition

$$\Phi_{p,\tau}^{\text{MS}} = \phi_{p,\tau} \quad \text{on } \partial\tau \setminus \Gamma_\varepsilon, \quad \Phi_{p,\tau}^{\text{MS}}(x_q) = \delta_{p,q} \quad \text{for all } p, q \in \mathcal{S}(\tau), \quad (2.4)$$

where  $\phi_{p,\tau}$  is the restriction of the standard linear nodal basis function  $\phi_p$  on  $\tau$ .

The flux  $\theta_{p,\tau_\varepsilon}$  is defined as follows. If  $\tau$  has no edge on  $\Gamma_\varepsilon$ , then we let  $\theta_{p,\tau} = 0$ . Problem (2.3) changes to a Dirichlet boundary value problem with a unique solution  $\Phi_{p,\tau}^{MS} = \phi_{p,\tau}$ , i.e., the multiscale basis function coincides with the linear basis function. If  $\tau_\varepsilon$  has one edge on  $\Gamma_\varepsilon$ , then

$$\theta_{p,\tau_\varepsilon}(x) := \begin{cases} \frac{\partial_n \phi_{p,\tau_0}}{r} & \text{if } \|g_\varepsilon - \langle g_\varepsilon \rangle\|_{L^\infty(\partial\tau_\varepsilon)} \leq C\varepsilon, \\ \frac{\partial_n \phi_{p,\tau_0}}{r} \frac{g_\varepsilon(x)}{\langle g_\varepsilon \rangle} & \text{otherwise.} \end{cases} \quad (2.5)$$

In this case, the local problem has mixed boundary conditions. Here the parameter  $r = |s_\varepsilon|/|s_0|$  with  $s_\varepsilon$  being the rough edge of  $\tau_\varepsilon$ , while  $s_0$  being the homogenized rough edge, and  $n$  is the unit outer normal of  $s_0$ ,  $\tau_0$  is the homogenized element of  $\tau_\varepsilon$  and  $\langle g_\varepsilon \rangle = \oint_{s_\varepsilon} g_\varepsilon$  is the mean of  $g_\varepsilon$  over  $s_\varepsilon$ .

The flux  $\theta_{p,\tau_\varepsilon}$  defined in (2.5)<sub>2</sub> contains both geometrical and physical information of the boundary. If the flux has no oscillations, i.e.,  $g_\varepsilon = \langle g_\varepsilon \rangle$ , then (2.5)<sub>2</sub> changes to (2.5)<sub>1</sub>, and the flux does not contain the physical information any more. Furthermore, if the boundary is also flat, i.e.,  $r = 1$ , then the unique solution of the cell problem is the linear nodal basis functions, and the method automatically changes to the standard finite element method.

The bound  $C\varepsilon$  in (2.5) is a threshold for determining whether the physical information should be incorporated into the cell problem. Roughly speaking, if  $\|g_\varepsilon - \langle g_\varepsilon \rangle\|_{L^\infty(\partial\tau_\varepsilon)}$  is as small as  $\mathcal{O}(\varepsilon)$ , then we need not any physical information but the geometrical information of the rough boundary. Otherwise, the physical information should be incorporated into the cell problem. This is consistent with our intuition as seen from the example below. If there is no information on  $\varepsilon$ , we can use (2.5)<sub>2</sub> whenever  $\langle g_\varepsilon \rangle \neq 0$ .

**EXAMPLE 2.1.** *If  $g_\varepsilon(x) = \varepsilon \sin(x/\varepsilon)$ , it is clear that  $\|g_\varepsilon - \langle g_\varepsilon \rangle\|_{L^\infty} = \varepsilon$ , then we may use (2.5)<sub>1</sub>. On the other hand, if  $g_\varepsilon(x) = 1 + \sin(x/\varepsilon)$ , then  $\|g_\varepsilon - \langle g_\varepsilon \rangle\|_{L^\infty} = 1$ , and we have to use (2.5)<sub>2</sub>. There are some special cases beyond (2.5), e.g.,  $g_\varepsilon(x) = \sin(x/\varepsilon)$  so that  $\|g_\varepsilon\|_\infty = 1$  but  $\langle g_\varepsilon \rangle = 0$ . In this case, the method works as well if we decompose  $g_\varepsilon$  as  $g_\varepsilon = g_1 + g_2$  with  $g_1 := 1$  and  $g_2 := \sin(x/\varepsilon) - 1$  and split Problem (2.1) into two problems with boundary conditions  $g_1$  and  $g_2$ , respectively. We would like to emphasize that this splitting technique does not apply to the nonlinear problems because the flux is not well-defined when  $\langle g_\varepsilon \rangle = 0$  and  $\|g_\varepsilon\|_{L^\infty} = \mathcal{O}(1)$ . Nevertheless, it may be directly applied to the corresponding linearized problems.*

Under the conditions (2.3), (2.4) and (2.5), we have, for all  $\tau \in \mathcal{T}_h$ ,

$$\sum_{p \in \mathcal{S}(\tau)} \Phi_{p,\tau}^{MS} = 1.$$

The basis function  $\phi_p^{MS}$  is continuous across the element boundary so that

$$V_h := \text{span} \{ \phi_p^{MS} \mid p \in \mathcal{S}(\Omega_\varepsilon) \} \subset V(\Omega_\varepsilon).$$

The MsFEM approximation of Problem (2.1) is to find  $u_h \in V_h$  such that

$$a(u_h, v) = (f, v) + (g_\varepsilon, v)_{\Gamma_\varepsilon} \quad \text{for all } v \in V_h. \quad (2.6)$$

This is a conforming method, and the existence and uniqueness of the solution follow from Lax-Milgram theorem. Moreover, we have

$$\|\nabla(u^\varepsilon - u_h)\|_{L^2(\Omega_\varepsilon)} = \inf_{v \in V_h} \|\nabla(u^\varepsilon - v)\|_{L^2(\Omega_\varepsilon)}. \quad (2.7)$$

The error estimate now boils down to the interpolate error estimate, which will be the focus of the later sections.

The MsFEM problem (2.6) has  $\mathcal{O}(h^{-2})$  freedoms in two dimension. To calculate each multiscale basis, we need  $\mathcal{O}(\tilde{h}^{-2})$  freedoms with  $\tilde{h}$  the mesh size of the local cell problem. The number of the cell problem is  $\mathcal{O}(h^{-1})$ . The overall complexity of the proposed method is of  $\mathcal{O}(h^{-2} + h^{-1}\tilde{h}^{-2})$ . Note that  $\tilde{h} \simeq M^{-1}h$ , the complexity is of  $\mathcal{O}(M^2h^{-3})$ . The cell problems are independent of each other, and could be solved in parallel.

REMARK 2.2. *The proposed method can be generalized to the problem with oscillatory inhomogeneous Dirichlet boundary conditions on the rough surface. We assume  $u^\varepsilon = g_\varepsilon$  on  $\Gamma_\varepsilon$ . The MsFEM basis functions  $\Phi_{p,\tau}^{MS}$  satisfy*

$$a_\tau(\Phi_{p,\tau}^{MS}, v) = 0 \quad \text{for all } v \in H_0^1(\tau), \quad (2.8)$$

*and is supplemented with the boundary condition:  $\Phi_{p,\tau}^{MS} = \theta_{p,\tau_\varepsilon}(x)$  on the rough edge  $\partial\tau \cap \Gamma_\varepsilon$  and  $\Phi_{p,\tau}^{MS} = \phi_{p,\tau}$  on  $\partial\tau \setminus \Gamma_\varepsilon$ , where*

$$\theta_{p,\tau_\varepsilon}(x) := \begin{cases} \frac{\phi_{p,\tau_0}}{r(x)} & \text{if } \|g_\varepsilon - \langle g_\varepsilon \rangle\|_{L^\infty(\partial\tau_\varepsilon)} \leq C\varepsilon, \\ \frac{\phi_{p,\tau_0}}{r(x)} \frac{g_\varepsilon(x)}{\langle g_\varepsilon \rangle(x)} & \text{otherwise,} \end{cases} \quad (2.9)$$

*The detailed analysis of the MsFEM for inhomogeneous Dirichlet boundary value problem will be addressed in a future paper.*

**3. Error Estimate for the Homogenization Problem.** In this section, we revisit some homogenization results for Problem (2.1), which have been established in [19], while we clarify the dependence of the estimates on the domain size, which is crucial for studying the accuracy of the proposed method. Our approach is different from that in [19] for estimate of the first order approximation.

We assume that  $\Omega_\varepsilon$  is given by

$$\Omega_\varepsilon := \{x \in \mathbb{R}^2 \mid 0 < x_1 < 1, \varepsilon\gamma(x_1/\varepsilon) < x_2 < 1\}, \quad (3.1)$$

and the oscillating bottom boundary  $\Gamma_\varepsilon$  is given by

$$\Gamma_\varepsilon = \{x \in \overline{\Omega}_\varepsilon \mid 0 < x_1 < 1, x_2 = \varepsilon\gamma(x_1/\varepsilon)\}$$

with  $\gamma$  a positive smooth 1-periodic function. We assume that  $g_\varepsilon(x_1) = g(x_1/\varepsilon)$  with  $g$  a smooth 1-periodic function and satisfying

$$\|g - \langle g \rangle\|_{L^\infty(\Sigma)} \leq C(|\langle g \rangle| + \varepsilon), \quad (3.2)$$

where  $\Sigma = \{ \xi \in \mathbb{R}^2 \mid 0 < \xi_1 < 1, \xi_2 = \gamma(\xi_1) \}$  with  $\langle g \rangle$  the mean of  $g$  over  $\Sigma$ :

$$\langle g \rangle = \frac{1}{r} \int_0^1 g(t) [1 + (\gamma'(t))^2]^{1/2} dt \quad \text{and} \quad r = \int_0^1 [1 + (\gamma'(t))^2]^{1/2} dt.$$

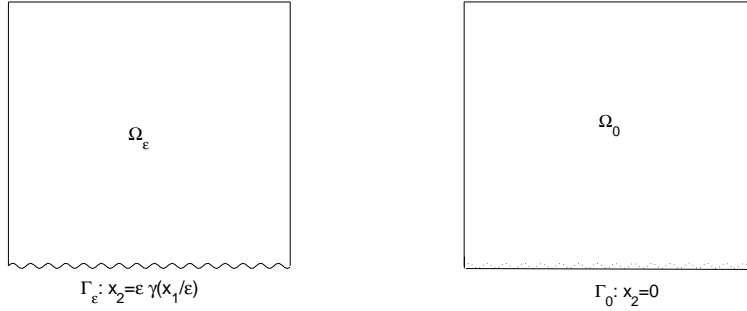


FIG. 3.1. The domains  $\Omega_\varepsilon$  and  $\Omega_0$ .

REMARK 3.1. The assumption  $\gamma \geq 0$  ensures  $\Omega_\varepsilon \subset \Omega_0$ . This may make the presentation slightly simpler. All the results in this section remain valid for general  $\gamma$ , we refer to [19, §8] and [36] for related discussions.

### 3.1. The zeroth order approximation. Let

$$\Omega_0 = \{ x \in \mathbb{R}^2 \mid 0 < x_1 < 1, 0 < x_2 < 1 \} \quad \text{and} \quad \Gamma_0 = \partial\Omega_0 \cap \{ x \in \mathbb{R}^2 \mid x_2 = 0 \}.$$

Define  $\Gamma_D := \partial\Omega_0 \setminus \Gamma_0$  and

$$V(\Omega_0) = \{ v \in H^1(\Omega_0) \mid v|_{\Gamma_D} = 0 \}.$$

The zeroth order approximations  $u^0$  of  $u^\varepsilon$  is such that  $u^0 \in V(\Omega_0)$  and

$$a_{\Omega_0}(u^0, v) = (f, v)_{\Omega_0} + (r\langle g \rangle, v)_{\Gamma_0} \quad \text{for all } v \in V(\Omega_0). \quad (3.3)$$

We start with an extension result that will be frequently used later on, which slightly refines that in [34, Appendix A].

LEMMA 3.2. There exists an extension operator  $E : H^1(\Omega_\varepsilon) \rightarrow H^1(\Omega_0)$  such that, for any  $\phi \in H^1(\Omega_\varepsilon)$ ,

$$\|E\phi\|_{H^1(\Omega_0)} \leq \sqrt{2 + 2A^2 + 2A\sqrt{1 + A^2}} \|\phi\|_{H^1(\Omega_\varepsilon)}, \quad (3.4)$$

where  $A = \|\gamma'\|_{L^\infty(0,1)}$ .

*Proof.* For any  $\phi \in H^1(\Omega_\varepsilon)$ , we define  $E\phi$  by reflection with respect to  $\Gamma_\varepsilon$ .

$$E\phi(x) = \begin{cases} \phi(x) & x \in \Omega_\varepsilon, \\ \phi(x_1, 2\varepsilon\gamma(x_1/\varepsilon) - x_2) & x \in \Omega_0 \setminus \Omega_\varepsilon. \end{cases}$$

A direct calculation gives

$$\partial_{x_1} E\phi(x) = \begin{cases} \partial_{x_1} \phi(x) & x \in \Omega_\varepsilon, \\ \partial_{x_1} \phi + 2\partial_{x_2} \phi \gamma'(x_1/\varepsilon) & x \in \Omega_0 \setminus \Omega_\varepsilon. \end{cases}$$

and

$$\partial_{x_2} E\phi(x) = \begin{cases} \partial_{x_2} \phi(x) & x \in \Omega_\varepsilon, \\ -\partial_{x_2} \phi(x_1, 2\varepsilon\gamma(x_1/\varepsilon) - x_2) & x \in \Omega_0 \setminus \Omega_\varepsilon. \end{cases}$$

Note the module of the Jacobian of the substitution

$$(x_1, x_2) \mapsto (x_1, 2\varepsilon\gamma(x_1/\varepsilon) - x_2)$$

is equal to one. Observe that the inequality

$$\|E\phi\|_{L^2(\Omega_0)}^2 \leq 2 \|\phi\|_{L^2(\Omega_\varepsilon)}^2$$

holds, where we have used

$$\begin{aligned} \|E\phi\|_{L^2(\Omega_0 \setminus \Omega_\varepsilon)}^2 &= \int_0^1 \int_0^{\varepsilon\gamma(x_1/\varepsilon)} |\phi(x_1, 2\varepsilon\gamma(x_1/\varepsilon) - x_2)|^2 dx \\ &= \int_0^1 \int_{\varepsilon\gamma(x_1/\varepsilon)}^{2\varepsilon\gamma(x_1/\varepsilon)} |\phi(x_1, x_2)|^2 dx \\ &\leq \|\phi\|_{L^2(\Omega_\varepsilon)}^2. \end{aligned}$$

Next, we estimate  $\partial_{x_1} E\phi$  and  $\partial_{x_2} E\phi$ .

$$\begin{aligned} \|\partial_{x_1} E\phi\|_{L^2(\Omega_0)}^2 &\leq \|\partial_{x_1} \phi\|_{L^2(\Omega_\varepsilon)}^2 + \|\partial_{x_1} \phi + 2\gamma' \partial_{x_2} \phi\|_{L^2(\Omega_\varepsilon)}^2 \\ &\leq (2+t) \|\partial_{x_1} \phi\|_{L^2(\Omega_\varepsilon)}^2 + 4A^2(1+1/t) \|\partial_{x_2} \phi\|_{L^2(\Omega_\varepsilon)}^2 \end{aligned}$$

with any  $t > 0$ , and

$$\|\partial_{x_2} E\phi\|_{L^2(\Omega_0)}^2 \leq 2 \|\partial_{x_2} \phi\|_{L^2(\Omega_\varepsilon)}^2.$$

The above three estimates imply

$$\|E\phi\|_{H^1(\Omega_0)}^2 \leq (2+t) \|\partial_{x_1} \phi\|_{L^2(\Omega_\varepsilon)}^2 + (2+4A^2(1+1/t)) \|\partial_{x_2} \phi\|_{L^2(\Omega_\varepsilon)}^2 + 2 \|\phi\|_{L^2(\Omega_\varepsilon)}^2.$$

Hence,

$$\|E\phi\|_{H^1(\Omega_0)}^2 \leq \max\{2+t, 2+4A^2(1+1/t)\} \|\phi\|_{H^1(\Omega_\varepsilon)}^2.$$



Optimizing the maximum with respect to parameter  $t$ , we obtain the maximum is minimal if  $t = 2A^2 + 2\sqrt{A^2 + A^4}$ . This completes the proof.  $\square$

To estimate the error between  $u^0$  and  $u^\varepsilon$ , we need an auxiliary result [39, Lemma 1.5, p.7]. The present form can be found in [38, inequality (17) in Lemma 10].

LEMMA 3.3. *Let  $\Omega$  be a Lipschitz domain, and  $S_\varepsilon := \{x \in \Omega \mid \text{dist}(x, \partial\Omega) \leq \varepsilon\}$ , then for any  $1/2 < \kappa \leq \mu \leq 1$  and  $v \in H^\mu(\Omega)$ , there holds*

$$\|v\|_{L^2(S_\varepsilon)} \leq C \left( \sqrt{\varepsilon} \|v\|_{H^\kappa(\Omega)} + \varepsilon^\mu \|v\|_{H^\mu(\Omega)} \right), \quad (3.5)$$

where  $C > 0$  is a constant independent of  $\varepsilon$ .

LEMMA 3.4. *Let  $u^\varepsilon$  and  $u^0$  be the solutions to Problems (2.1) and (3.3), respectively. Then*

$$\|\nabla(u^\varepsilon - u^0)\|_{L^2(\Omega_\varepsilon)} \leq C\sqrt{\varepsilon}(\|f\|_{L^2(\Omega_0)} + \|\nabla u^0\|_{H^1(\Omega_0)} + \|g_\varepsilon\|_{L^2(\Gamma_\varepsilon)}). \quad (3.6)$$

*Proof.* Denote  $e = u^\varepsilon - u^0 \in V(\Omega_\varepsilon)$ . For any  $\phi \in V(\Omega_\varepsilon)$ , we have

$$\begin{aligned} \int_{\Omega_\varepsilon} \nabla e \nabla \phi \, dx &= - \int_{\Omega_0 \setminus \Omega_\varepsilon} (f\phi - \nabla u^0 \cdot \nabla \phi) \, dx + \int_{\Gamma_\varepsilon} g_\varepsilon \phi \, d\sigma(x) - \int_{\Gamma_0} r \langle g \rangle \phi \, dx_1 \\ &= - \int_{\Omega_0 \setminus \Omega_\varepsilon} (f\phi - \nabla u^0 \cdot \nabla \phi) \, dx \\ &\quad + \int_0^1 \left( g(x_1/\varepsilon) \phi(x_1, \varepsilon \gamma(x_1/\varepsilon)) [1 + (\gamma'(x_1/\varepsilon))^2]^{1/2} - r \langle g \rangle \phi(x_1, 0) \right) dx_1 \\ &= I_1 + I_2. \end{aligned}$$

Using (3.5), we bound  $I_1$  as

$$\begin{aligned} |I_1| &\leq \|f\|_{L^2(\Omega_0 \setminus \Omega_\varepsilon)} \|\phi\|_{L^2(\Omega_0 \setminus \Omega_\varepsilon)} + \|\nabla u^0\|_{L^2(\Omega_0 \setminus \Omega_\varepsilon)} \|\nabla \phi\|_{L^2(\Omega_0 \setminus \Omega_\varepsilon)} \\ &\leq C\sqrt{\varepsilon} \|f\|_{L^2(\Omega_0)} \|\phi\|_{H^1(\Omega_0)} + C\sqrt{\varepsilon} \|\nabla u^0\|_{H^1(\Omega_0)} \|\nabla \phi\|_{L^2(\Omega_0)} \\ &\leq C\sqrt{\varepsilon} \left( \|f\|_{L^2(\Omega_0)} + \|\nabla u^0\|_{H^1(\Omega_0)} \right) \|\nabla \phi\|_{L^2(\Omega_0)}, \end{aligned} \quad (3.7)$$

where in the last step we have used *Poincaré's inequality* for  $\phi$ .

Denote by  $p^\varepsilon(x_1) = p(x_1/\varepsilon)$  with  $p(t) = g(t)[1 + \gamma'(t)^2]^{1/2}$ , we have

$$I_2 = \int_0^1 (p^\varepsilon(x_1) \phi(x_1, \varepsilon \gamma(x_1/\varepsilon)) - \langle p \rangle \phi(x_1, 0)) \, dx_1,$$

where  $\langle p \rangle$  denotes the average of  $p$  and  $\langle p \rangle = r \langle g \rangle$ , i.e.,  $\langle p \rangle = \int_0^1 g(t)[1 + \gamma'(t)^2]^{1/2} \, dt$ .

It is clear to see

$$I_2 = \int_0^1 p^\varepsilon(x_1) (\phi(x_1, \varepsilon \gamma(x_1/\varepsilon)) - \phi(x_1, 0)) \, dx_1 + \int_0^1 (p^\varepsilon - \langle p \rangle) \phi(x_1, 0) \, dx_1.$$

A direct calculation gives that

$$\begin{aligned}
\left| \int_0^1 p^\varepsilon(x_1) (\phi(x_1, \varepsilon\gamma(x_1/\varepsilon)) - \phi(x_1, 0)) \, dx_1 \right| &= \left| \int_0^1 p^\varepsilon(x_1) \int_0^{\varepsilon\gamma(x_1/\varepsilon)} \frac{\partial \phi}{\partial x_2} \, dx_2 \, dx_1 \right| \\
&\leq \sqrt{\varepsilon} \|\nabla \phi\|_{L^2(\Omega_0 \setminus \Omega_\varepsilon)} \left\| p^\varepsilon \gamma^{1/2} \right\|_{L^2(\Gamma_0)} \\
&\leq C \sqrt{\varepsilon} \|\nabla \phi\|_{L^2(\Omega_0)} \|g_\varepsilon\|_{L^2(\Gamma_\varepsilon)},
\end{aligned}$$

where we have used

$$\left\| p^\varepsilon \gamma^{1/2} \right\|_{L^2(\Gamma_0)}^2 \leq A \|\gamma\|_{L^\infty(0,1)} \|g_\varepsilon\|_{L^2(\Gamma_\varepsilon)}^2.$$

Denote by  $s_0 = 0 < s_1 = \varepsilon < \dots < s_N = N\varepsilon = 1$ , using the fact that

$$\langle p \rangle = \langle p^\varepsilon \rangle_i = \int_{s_i}^{s_{i+1}} p^\varepsilon(x_1) \, dx_1,$$

we decompose the second term into

$$\int_{\Gamma_0} (p^\varepsilon(x_1) - \langle p \rangle) \phi(x_1, 0) \, dx_1 = \sum_{i=0}^{N-1} \int_{s_i}^{s_{i+1}} p^\varepsilon(x_1) (\phi(x_1, 0) - \langle \phi \rangle_i) \, dx_1,$$

where  $\langle \phi \rangle_i = \int_{s_i}^{s_{i+1}} \phi(x_1, 0) \, dx_1$ . Using *Poincaré's inequality*, we obtain

$$\begin{aligned}
\left| \int_{\Gamma_0} (p^\varepsilon(x_1) - \langle p \rangle) \phi(x_1, 0) \, dx_1 \right| &\leq \sum_{i=0}^{N-1} \|p^\varepsilon\|_{L^2(s_i, s_{i+1})} \|\phi - \langle \phi \rangle_i\|_{L^2(s_i, s_{i+1})} \\
&\leq C \sqrt{\varepsilon} \sum_{i=0}^{N-1} \|p^\varepsilon\|_{L^2(s_i, s_{i+1})} \|\phi\|_{H^{1/2}(s_i, s_{i+1})} \\
&\leq C \sqrt{\varepsilon} \left( \sum_{i=0}^{N-1} \|p^\varepsilon\|_{L^2(s_i, s_{i+1})}^2 \right)^{1/2} \left( \sum_{i=0}^{N-1} \|\phi\|_{H^{1/2}(s_i, s_{i+1})}^2 \right)^{1/2} \\
&\leq C \sqrt{\varepsilon} \|g_\varepsilon\|_{L^2(\Gamma_\varepsilon)} \|\phi\|_{H^{1/2}(\Gamma_0)} \\
&\leq C \sqrt{\varepsilon} \|g_\varepsilon\|_{L^2(\Gamma_\varepsilon)} \|\phi\|_{H^1(\Omega_0)},
\end{aligned}$$

where we have used the fact that  $\sum_{i=0}^{N-1} \|p^\varepsilon\|_{L^2(s_i, s_{i+1})}^2 \leq (1+A) \|g_\varepsilon\|_{L^2(\Gamma_\varepsilon)}^2$ . This implies

$$|I_2| \leq C \sqrt{\varepsilon} \|\phi\|_{H^1(\Omega_0)} \|g_\varepsilon\|_{L^2(\Gamma_\varepsilon)}. \quad (3.8)$$

Using the extension result (3.4), we have

$$\|u^\varepsilon - u^0\|_{H^1(\Omega_0)} \leq C \|u^\varepsilon - u^0\|_{H^1(\Omega_\varepsilon)},$$

where  $C$  only depends on  $\|\gamma'\|_{L^\infty(0,1)}$ . This inequality together with (3.7) and (3.8) implies (3.6).  $\square$

The above lemma shows that  $u^0$  approximates to  $u^\varepsilon$  in  $H^1$  seminorm with rate  $\mathcal{O}(\sqrt{\varepsilon})$ . The convergence rate is inadequate in many applications. We step to the first order approximation in the next part.

**3.2. Some auxiliary problems.** To find the next order approximation of Problem (2.1), we define a semi-infinite tube as

$$Z_{bl} = \{ \xi \in \mathbb{R}^2 \mid 0 < \xi_1 < 1, \xi_2 > \gamma(\xi_1) \}$$

with a curved boundary  $\Sigma = \{ \xi \in \mathbb{R}^2 \mid 0 < \xi_1 < 1, \xi_2 = \gamma(\xi_1) \}$ .

Three auxiliary problems are defined as follows. Let  $\beta_0, \beta_1$  and  $\beta_2$  be three unknown functions posed on  $Z_{bl}$ , which are periodic in  $\xi_1$  with period 1 and satisfy

$$\begin{cases} -\Delta_\xi \beta_0 = 0, & \text{in } Z_{bl}, \\ \frac{\partial \beta_0}{\partial n} = g(\xi_1) - \langle g \rangle, & \text{on } \Sigma, \\ \lim_{\xi_2 \rightarrow \infty} \beta_0 = 0, \end{cases} \quad (3.9)$$

and

$$\begin{cases} -\Delta_\xi \beta_1 = 0, & \text{in } Z_{bl}, \\ \frac{\partial \beta_1}{\partial n} = -\frac{\gamma'(\xi_1)}{[1 + (\gamma'(\xi_1))^2]^{1/2}}, & \text{on } \Sigma, \\ \lim_{\xi_2 \rightarrow \infty} \beta_1 = 0, \end{cases} \quad (3.10)$$

and

$$\begin{cases} -\Delta_\xi \beta_2 = 0, & \text{in } Z_{bl}, \\ \frac{\partial \beta_2}{\partial n} = \frac{1}{[1 + (\gamma'(\xi_1))^2]^{1/2}} - \frac{1}{r}, & \text{on } \Sigma, \\ \lim_{\xi_2 \rightarrow \infty} \beta_2 = 0. \end{cases} \quad (3.11)$$

Here  $\Delta_\xi = \partial_{\xi_1}^2 + \partial_{\xi_2}^2$ . It is well-known that each problem has a unique solution, and the solutions have the following decay properties [19, Theorem 2.2]. Similar results for Dirichlet boundary value problems can also be found in [3, 35].

**LEMMA 3.5.** *Let  $\beta_0, \beta_1$  and  $\beta_2$  be the solutions of (3.9), (3.10) and (3.11), respectively. Then, for  $i = 0, 1$  and  $2$ , there exist constants  $C$  and  $\delta$  such that*

$$\|\beta_i\|_{L^\infty(Z_{bl})} + \|\nabla_\xi \beta_i\|_{L^\infty(Z_{bl})} \leq C e^{-\delta \xi_2}. \quad (3.12)$$

**3.3. The first order approximation.** Denote  $\beta_i^\varepsilon(x) = \beta_i(x/\varepsilon)$  for  $i = 0, 1, 2$ , and define

$$u^1(x) = \beta_0^\varepsilon(x) + \beta_i^\varepsilon \partial_{x_i} u^0(x). \quad (3.13)$$

The first order approximation  $u_1^\varepsilon = u^0 + \varepsilon u^1$ , which does not satisfy the homogeneous Dirichlet boundary condition as  $u^\varepsilon$  on  $\Gamma_D$ . It is useful to introduce a corrector  $u^{cr}$  to the first order approximation, which satisfies  $u^{cr} - u^1 \in V(\Omega_0)$  and

$$a_{\Omega_0}(u^{cr}, v) = 0 \quad \text{for all } v \in V(\Omega_0). \quad (3.14)$$

The corrector  $u^{cr}$  can be estimated as follows.

LEMMA 3.6. *Let  $u^{cr}$  be the solution of (3.14), then there exists  $C$  that is independent of the size of  $\Omega_0$  such that*

$$\|\nabla u^{cr}\|_{L^2(\Omega_0)} \leq C \left(1 + \|\nabla u^0\|_{L^\infty(\Omega_0)} + \|\nabla^2 u^0\|_{L^2(\Omega_0)}\right). \quad (3.15)$$

*Proof.* Define a smooth cut-off function  $\rho_\varepsilon \in C_0^\infty(\Omega_0)$  by

$$\rho_\varepsilon(x) = \begin{cases} 1, & x \in \Omega_0, \text{dist}(x, \Gamma_D) \geq 2\varepsilon, \\ 0, & x \in \Omega_0, \text{dist}(x, \Gamma_D) \leq \varepsilon, \end{cases}$$

and  $\|\rho_\varepsilon\|_{L^\infty(\Omega_0)} \leq 1$  and  $\|\nabla \rho_\varepsilon\|_{L^\infty(\Omega_0)} \leq C/\varepsilon$ .

Let  $\eta^\varepsilon(x) = (1 - \rho_\varepsilon(x))u^1(x)$ . It is clear to see

$$\|\nabla u^{cr}\|_{L^2(\Omega_0)} \leq \|\nabla \eta^\varepsilon\|_{L^2(\Omega_0)}.$$

A direct calculation gives

$$\frac{\partial \eta^\varepsilon}{\partial x_i} = -\partial_{x_i} \rho_\varepsilon u^1 + (1 - \rho_\varepsilon) \beta_j^\varepsilon \partial_{x_i x_j}^2 u^0 + (1 - \rho_\varepsilon) (\partial_{x_i} \beta_0^\varepsilon + \partial_{x_i} \beta_j^\varepsilon \partial_{x_j} u^0).$$

Using the decay estimate for  $\beta_i^\varepsilon$  in Lemma 3.5, we may bound  $\|\nabla \eta^\varepsilon\|_{L^2(\Omega_0)}$  as follows. We only estimate the first term, other terms can be bounded similarly.

$$\begin{aligned} \|\partial_{x_i} \rho_\varepsilon \beta_0^\varepsilon\|_{L^2(\Omega_0)}^2 &\leq C\varepsilon^{-2} \left( \int_\varepsilon^{2\varepsilon} + \int_{1-2\varepsilon}^{1-\varepsilon} \right) \int_0^\infty e^{-2\delta x_2/\varepsilon} dx + C\varepsilon^{-2} \int_0^1 \int_{1-2\varepsilon}^{1-\varepsilon} e^{-2\delta x_2/\varepsilon} dx \\ &\leq C\varepsilon^{-2} \left( \varepsilon^2 + \varepsilon e^{-2\delta/\varepsilon} \right) \leq C, \end{aligned}$$

where we have used (3.12) and the fact that  $\rho_\varepsilon$  supports in a narrow layer of width  $\mathcal{O}(\varepsilon)$ . Similarly, we have

$$\begin{aligned} \|\partial_{x_i} \rho_\varepsilon \partial_{x_j} u^0 \beta_j^\varepsilon\|_{L^2(\Omega_0)} &\leq C \|\nabla u^0\|_{L^\infty(\Omega_0)}, \\ \|(1 - \rho_\varepsilon) \partial_{x_i x_j}^2 u^0 \beta_j^\varepsilon\|_{L^2(\Omega_0)} &\leq C \|\nabla^2 u^0\|_{L^2(\Omega_0)}, \\ \|(1 - \rho_\varepsilon) \partial_{x_i} \beta_0^\varepsilon\|_{L^2(\Omega_0)} &\leq C, \\ \|(1 - \rho_\varepsilon) \partial_{x_j} u^0 \partial_{x_i} \beta_j^\varepsilon\|_{L^2(\Omega_0)} &\leq C \|\nabla u^0\|_{L^\infty(\Omega_0)}. \end{aligned}$$

Summing up all the terms, we obtain (3.15) and complete the proof.  $\square$

The next theorem gives the error estimate for the first order approximation.

THEOREM 3.7. *Let  $u^\varepsilon$  and  $u_0$  be the solutions of Problems (2.1) and (3.3), respectively. Let  $u^1$  be defined in (3.13). There exists  $C$  independent of the size of  $\Omega_0$  such that*

$$\|\nabla(u^\varepsilon - u_1^\varepsilon)\|_{L^2(\Omega_\varepsilon)} \leq C\varepsilon(1 + \|\nabla u^0\|_{W^{1,\infty}(\Omega_0)} + \|\nabla^2 u^0\|_{H^1(\Omega_0)}). \quad (3.16)$$

*Proof.* For any  $v \in V(\Omega_\varepsilon)$ , an integration by parts yields

$$\int_{\Omega_\varepsilon} \nabla u^0 \nabla v \, dx = \int_{\Omega_\varepsilon} f v \, dx + \int_{\Gamma_\varepsilon} \frac{\partial u^0}{\partial n} v \, d\sigma(x),$$

which together with (2.2) gives

$$\int_{\Omega_\varepsilon} \nabla(u^\varepsilon - u^0) \nabla v \, dx = \int_{\Gamma_\varepsilon} \left( g_\varepsilon - \frac{\partial u^0}{\partial n} \right) v \, d\sigma(x). \quad (3.17)$$

Next we calculate  $\int_{\Omega_\varepsilon} \nabla u^1 \nabla v \, dx$ . Under the change of variables  $\xi = x/\varepsilon$ ,  $\Omega_\varepsilon$  is mapped onto a domain

$$D_{\varepsilon,\xi} := \{ \xi \in \mathbb{R}^2 \mid 0 < \xi_1 < 1/\varepsilon, \gamma(\xi_1) < \xi_2 < 1/\varepsilon \}$$

with the curved boundary  $\Gamma_{\varepsilon,\xi} := \{ \xi \in \mathbb{R}^2 \mid 0 < \xi_1 < 1/\varepsilon, \xi_2 = \gamma(\xi_1) \}$ . We denote  $D_{0,\xi}$  as the mapped domain of  $\Omega_0$  under this map. Notice that for any function  $v$ ,

$$D_x v = \nabla_x v + \frac{1}{\varepsilon} \nabla_\xi v.$$

Clearly,

$$\int_{\Omega_\varepsilon} \nabla u^1 \nabla v \, dx = \int_{\Omega_\varepsilon} \nabla_x u^1 \nabla v \, dx + \int_{D_{\varepsilon,\xi}} \nabla_\xi u^1 \nabla_\xi v \, d\xi.$$

A direct calculation gives

$$\begin{aligned} \int_{D_{\varepsilon,\xi}} \nabla_\xi u^1 \nabla_\xi v \, d\xi &= \int_{D_{\varepsilon,\xi}} \left( \nabla_\xi \beta_0 \nabla_\xi v + \nabla_\xi \beta_i \nabla_\xi \left( \frac{\partial u^0}{\partial x_i} v \right) \right) d\xi \\ &\quad + \int_{D_{\varepsilon,\xi}} \frac{\partial}{\partial x_i} (\nabla_\xi u^0) (\beta_i \nabla_\xi v - v \nabla_\xi \beta_i) \, d\xi. \end{aligned}$$

Using the definition of  $\{\beta_i\}_{i=0}^2$ , an integration by parts yields

$$\int_{D_{\varepsilon,\xi}} \nabla_\xi \beta_0 \nabla_\xi v \, d\xi = \int_{\Gamma_{\varepsilon,\xi}} (g - \langle g \rangle) v \, d\sigma(\xi),$$

and

$$\begin{aligned} \int_{D_{\varepsilon,\xi}} \nabla_\xi \beta_i \nabla_\xi \left( \frac{\partial u^0}{\partial x_i} v \right) d\xi &= - \int_{\Gamma_{\varepsilon,\xi}} \left( n_\xi^1 \frac{\partial u^0}{\partial x_1} + n_\xi^2 \frac{\partial u^0}{\partial x_2} \right) v \, d\sigma(\xi) - \frac{1}{r} \int_{\Gamma_{\varepsilon,\xi}} \frac{\partial u^0}{\partial x_2} v \, d\sigma(\xi) \\ &= - \frac{1}{\varepsilon} \int_{\Gamma_{\varepsilon,\xi}} \frac{\partial u^0}{\partial n_\xi} v \, d\sigma(\xi) - \frac{1}{r\varepsilon} \int_{\Gamma_{\varepsilon,\xi}} \frac{\partial u^0}{\partial \xi_2} v \, d\sigma(\xi). \end{aligned}$$

Using the fact that  $\partial u^0 / \partial n = r \langle g \rangle$  on  $\Gamma_0$ , we rewrite the last term in the right-hand side of the above identity as

$$\begin{aligned} - \frac{1}{r\varepsilon} \int_{\Gamma_{\varepsilon,\xi}} \frac{\partial u^0}{\partial \xi_2} v \, d\sigma(\xi) &= - \frac{1}{r\varepsilon} \int_{\Gamma_{\varepsilon,\xi}} \frac{\partial u^0}{\partial \xi_2} (\xi_1, 0) v \, d\sigma(\xi) \\ &\quad - \frac{1}{r\varepsilon} \int_{\Gamma_{\varepsilon,\xi}} \left( \frac{\partial u^0}{\partial \xi_2} (\xi_1, \gamma(\xi_1)) - \frac{\partial u^0}{\partial \xi_2} (\xi_1, 0) \right) v \, d\sigma(\xi) \\ &= \int_{\Gamma_{\varepsilon,\xi}} \langle g \rangle v \, d\sigma(\xi) - \frac{1}{r\varepsilon} \int_{D_{0,\xi} \setminus D_{\varepsilon,\xi}} \frac{\partial^2 u^0}{\partial \xi_2^2} d\xi. \end{aligned}$$

Combining the above three equations, we obtain

$$\begin{aligned} \int_{D_{\varepsilon,\xi}} \nabla_{\xi} u^1 \nabla_{\xi} v \, d\xi &= \int_{\Gamma_{\varepsilon,\xi}} \left( g - \frac{1}{\varepsilon} \frac{\partial u^0}{\partial n_{\xi}} \right) v \, d\sigma(\xi) \\ &+ \int_{D_{\varepsilon,\xi}} \frac{\partial}{\partial x_i} (\nabla_{\xi} u^0) (\beta_i \nabla_{\xi} v - v \nabla_{\xi} \beta_i) \, d\xi - \frac{1}{r\varepsilon} \int_{D_{0,\xi} \setminus D_{\varepsilon,\xi}} v \frac{\partial^2 u^0}{\partial \xi_2^2} \, d\xi. \end{aligned}$$

Denote  $e = u^{\varepsilon} - u^0 - \varepsilon u^1 - \varepsilon u^{\text{cr}}$ , we have the following error expansion:

$$\begin{aligned} \int_{\Omega_{\varepsilon}} \nabla e \nabla v \, dx &= \frac{1}{r} \int_{\Omega_0 \setminus \Omega_{\varepsilon}} \frac{\partial^2 u^0}{\partial x_2^2} v \, dx - \varepsilon \int_{\Omega_{\varepsilon}} \nabla_x u^1 \nabla v \, dx - \varepsilon \int_{\Omega_{\varepsilon}} \nabla u^{\text{cr}} \nabla v \, dx \\ &- \int_{D_{\varepsilon,\xi}} \frac{\partial}{\partial \xi_i} (\nabla_{\xi} u^0) (\beta_i \nabla_{\xi} v - v \nabla_{\xi} \beta_i) \, d\xi. \end{aligned}$$

By Lemma 3.3, we obtain

$$\left| \frac{1}{r} \int_{\Omega_0 \setminus \Omega_{\varepsilon}} \frac{\partial^2 u^0}{\partial x_2^2} v \, dx \right| \leq C\varepsilon \|\nabla^2 u^0\|_{H^1(\Omega_0)} \|v\|_{H^1(\Omega_0)}.$$

The second term can be bounded as

$$\left| \varepsilon \int_{\Omega_{\varepsilon}} \nabla_x u^1 \nabla v \, dx \right| \leq \varepsilon \|\nabla_x u^1\|_{L^2(\Omega_{\varepsilon})} \|\nabla v\|_{L^2(\Omega_{\varepsilon})} \leq C\varepsilon \|\nabla^2 u^0\|_{L^2(\Omega_{\varepsilon})} \|\nabla v\|_{L^2(\Omega_{\varepsilon})},$$

where  $C$  depends on  $\|\beta_i\|_{L^{\infty}}$ , which are uniformly bounded.

We transform the last integrand back to  $\Omega_{\varepsilon}$  as

$$\int_{D_{\varepsilon,\xi}} \frac{\partial}{\partial \xi_i} (\nabla_{\xi} u^0) (\beta_i \nabla_{\xi} v - v \nabla_{\xi} \beta_i) \, d\xi = \varepsilon \int_{\Omega_{\varepsilon}} \frac{\partial}{\partial x_i} (\nabla_x u^0) (\beta_i \nabla_x v - v \nabla_x \beta_i) \, dx.$$

The first term can be bounded as

$$\varepsilon \left| \int_{\Omega_{\varepsilon}} \frac{\partial}{\partial x_i} (\nabla_x u^0) \beta_i \nabla_x v \, dx \right| \leq \varepsilon \max_i \|\beta_i\|_{L^{\infty}} \|\nabla^2 u^0\|_{L^2(\Omega_{\varepsilon})} \|\nabla v\|_{L^2(\Omega_{\varepsilon})}.$$

By Lemma 3.5, we bound the second term as

$$\begin{aligned} \varepsilon \left| \int_{\Omega_{\varepsilon}} \frac{\partial}{\partial x_i} (\nabla_x u^0) v \nabla_x \beta_i \, dx \right| &\leq C \|\nabla^2 u^0\|_{L^{\infty}(\Omega_{\varepsilon})} \int_{\Omega_{\varepsilon}} e^{-\delta x_2/\varepsilon} |v| \, dx \\ &\leq C \|\nabla^2 u^0\|_{L^{\infty}(\Omega_{\varepsilon})} \int_0^{\infty} e^{-\delta x_2/\varepsilon} \int_0^1 |v| \, dx_1 \, dx_2. \end{aligned}$$

By trace inequality, for any  $x_2 \in (0, 1)$ , we have

$$\int_0^1 |v(x_1, x_2)| \, dx_1 \leq C \|v\|_{H^1(\Omega_{\varepsilon})}.$$

Combining the above two inequalities, we obtain

$$\varepsilon \left| \int_{\Omega_{\varepsilon}} \frac{\partial}{\partial x_i} (\nabla_x u^0) v \nabla_x \beta_i \, dx \right| \leq C\varepsilon \|\nabla^2 u^0\|_{L^{\infty}(\Omega_{\varepsilon})} \|v\|_{H^1(\Omega_{\varepsilon})}.$$

Summing up all the estimates, we obtain that for any  $v \in V_0(\Omega_\varepsilon)$ ,

$$\begin{aligned} \left| \int_{\Omega_\varepsilon} \nabla e \nabla v \, dx \right| &\leq C\varepsilon \left( \|\nabla^2 u^0\|_{H^1(\Omega_0)} + \|\nabla^2 u^0\|_{L^\infty(\Omega_\varepsilon)} + 1 \right) \|v\|_{H^1(\Omega_0)} \\ &\quad + \varepsilon \|\nabla u^{\text{cr}}\|_{L^2(\Omega_\varepsilon)} \|\nabla v\|_{L^2(\Omega_\varepsilon)}. \end{aligned} \quad (3.18)$$

Since  $\Gamma_\varepsilon$  is uniformly Lipschitz, we can extend  $u^\varepsilon$  from  $\Omega_\varepsilon$  to  $\Omega_0$  so that

$$\|e\|_{H^1(\Omega_0)} \leq C \|e\|_{H^1(\Omega_\varepsilon)},$$

where  $C$  only depends on  $\|h'\|_{L^\infty(Y)}$  by Lemma 3.2. Taking  $v = e$  in (3.18), we obtain

$$\|\nabla e\|_{L^2(\Omega_\varepsilon)}^2 \leq C\varepsilon \left( \|\nabla^2 u^0\|_{H^1(\Omega_0)} + \|\nabla^2 u^0\|_{L^\infty(\Omega_\varepsilon)} + 1 + \|\nabla u^{\text{cr}}\|_{L^2(\Omega_\varepsilon)} \right) \|e\|_{H^1(\Omega_\varepsilon)}.$$

Using Poincaré's inequality to  $e$  because  $e \in V_0(\Omega_\varepsilon)$ , we obtain

$$\|\nabla e\|_{L^2(\Omega_\varepsilon)} \leq C\varepsilon \left( \|\nabla^2 u^0\|_{H^1(\Omega_0)} + \|\nabla^2 u^0\|_{L^\infty(\Omega_\varepsilon)} + 1 + \|\nabla u^{\text{cr}}\|_{L^2(\Omega_\varepsilon)} \right),$$

which together with (3.15) yields the desired estimate (3.16).  $\square$

**4. Error Estimate.** We are ready to prove the convergence rate of the proposed MsFEM by the homogenization results in the last section. For any element  $\tau_\varepsilon$  with a rough side on  $\Gamma_\varepsilon$ , we assume that  $\tau_\varepsilon$  is contained in its homogenized domain  $\tau_0$ . Given this assumption, we could apply Theorem 3.7 to each element. In fact, this seemingly restrictive assumption is not essential because Theorem 3.7 remains valid without such assumption. Therefore, the error estimate also holds true without this assumption, which is also confirmed by the numerical examples in the next section. In addition, to avoid too many technical complexity, the estimate is restricted to the triangular element, while the proof can be generalized to the quadrilateral element with minor modifications.

**4.1. Homogenization of multiscale basis functions.** We start with some homogenization results of the multiscale basis functions  $\Phi_{p,\tau_\varepsilon}^{\text{MS}}$ . By the homogenization results in last section, we may clarify the zeroth order approximation and the first order approximation of  $\Phi_{p,\tau_\varepsilon}^{\text{MS}}$ , which are denoted by  $\Phi_{p,\tau_\varepsilon}^0$  and  $\Phi_{p,\tau_\varepsilon}^1$ , respectively.

Note that  $\Phi_{p,\tau_\varepsilon}^0 - \phi_{p,\tau_0} \in V_0(\tau_0)$  and

$$a_{\tau_0}(\Phi_{p,\tau_\varepsilon}^0, v) = (r\langle \theta \rangle_{p,\tau_\varepsilon}, v)_{\partial\tau_0 \cap \Gamma_0} \quad \text{for all } v \in V_0(\tau_0).$$

It is clear  $r\langle \theta \rangle_{p,\tau_\varepsilon} = \partial_n \phi_{p,\tau_0}$ . We conclude that the unique solution of the above problem is  $\Phi_{p,\tau_\varepsilon}^0 = \phi_{p,\tau_0}$ .

The first order corrector  $\Phi_{p,\tau_\varepsilon}^1$  of  $\Phi_{p,\tau_\varepsilon}^{\text{MS}}$  is given by

$$\Phi_{p,\tau_\varepsilon}^1 = \tilde{\beta}_0^\varepsilon \partial_n \phi_{p,\tau_0} + \beta_i^\varepsilon \frac{\partial \phi_{p,\tau_0}}{\partial x_i},$$

where  $\tilde{\beta}_0^\varepsilon(x) = \tilde{\beta}_0(x/\varepsilon)$  with  $\tilde{\beta}_0$  being the solution of

$$\begin{cases} -\Delta_\xi \tilde{\beta}_0 = 0, & \text{in } Z_{bl}, \\ \partial_n \tilde{\beta}_0 = \frac{1}{r} \left( g(\xi_1) / \langle g \rangle - 1 \right), & \text{on } \Sigma, \\ \lim_{\xi_2 \rightarrow \infty} \tilde{\beta}_0 = 0. \end{cases}$$

It is clear that  $\tilde{\beta}_0 = 0$  if  $g = \langle g \rangle$ . When  $\tilde{\beta}_0 = 0$ , the proof is simpler than the case  $\tilde{\beta}_0 \neq 0$  but the estimate is same. We only consider the later case in the following.

For any  $\tau \in \mathcal{T}_h$ , we define the MsFEM interpolant of  $u^\varepsilon$  as

$$\Pi_h u^\varepsilon := \sum_{p \in \mathcal{S}(\tau)} u^0(x_p) \Phi_{p, \tau_\varepsilon}^{\text{MS}}.$$

It is clear to see  $\Pi_h u^\varepsilon$  reduces to the standard linear Lagrange interpolant of  $u^0$ , which is denoted by  $\pi_h u^0$  when  $\tau$  has no side on  $\Gamma_\varepsilon$ . For element  $\tau_\varepsilon$  with a rough side, we define the first-order approximation of the MsFEM interpolant by

$$(\Pi_h u^\varepsilon)_1 := \sum_{p \in \mathcal{S}(\tau_\varepsilon)} u^0(x_p) (\phi_{p, \tau_0} + \varepsilon \Phi_{p, \tau_\varepsilon}^1).$$

The interpolate estimate is based on the following decomposition

$$u^\varepsilon - \Pi_h u^\varepsilon = (u^\varepsilon - u_1^\varepsilon) + (u_1^\varepsilon - (\Pi_h u^\varepsilon)_1) + ((\Pi_h u^\varepsilon)_1 - \Pi_h u^\varepsilon). \quad (4.1)$$

The following lemma is a direct consequence of Theorem 3.7.

LEMMA 4.1. *For any rough-sided element  $\tau_\varepsilon$ , we have*

$$\|\nabla \Pi_h u^\varepsilon - \nabla (\Pi_h u^\varepsilon)_1\|_{L^2(\tau_\varepsilon)} \leq C\varepsilon(1 + \|\nabla u^0\|_{L^\infty(\tau_0)}). \quad (4.2)$$

By definition, we rewrite  $(\Pi_h u^\varepsilon)_1$  as

$$(\Pi_h u^\varepsilon)_1 = \pi_h u^0 + \varepsilon \tilde{\beta}_0^\varepsilon \frac{\partial \pi_h u^0}{\partial n} + \varepsilon \beta_i^\varepsilon \frac{\partial \pi_h u^0}{\partial x_i}, \quad (4.3)$$

and

$$u_1^\varepsilon = u^0 + \varepsilon \tilde{\beta}_0^\varepsilon \frac{\partial u^0}{\partial n} + \varepsilon \beta_i^\varepsilon \frac{\partial u^0}{\partial x_i}. \quad (4.4)$$

A direct consequence of the representations (4.3) and (4.4) is

LEMMA 4.2. *For any rough-sided element  $\tau_\varepsilon$ , we have*

$$\|\nabla u_1^\varepsilon - \nabla (\Pi_h u^\varepsilon)_1\|_{L^2(\tau_\varepsilon)} \leq C(h_{\tau_\varepsilon} + \varepsilon) \|D^2 u^0\|_{L^2(\tau_\varepsilon)}.$$



*Proof.* A direct calculation gives that for  $i = 1, 2$ ,

$$\begin{aligned} \frac{\partial}{\partial x_i} (u_1^\varepsilon - \nabla(\Pi_h u^\varepsilon)_1) &= \frac{\partial}{\partial x_i} (u^0 - \pi_h u^0) + \varepsilon \frac{\partial \tilde{\beta}_0^\varepsilon}{\partial x_i} \frac{\partial}{\partial n} (u^0 - \pi_h u^0) \\ &\quad + \varepsilon \tilde{\beta}_0^\varepsilon \frac{\partial^2 u^0}{\partial n \partial x_i} + \varepsilon \frac{\partial \beta_j^\varepsilon}{\partial x_i} \frac{\partial}{\partial x_j} (u^0 - \pi_h u^0) + \varepsilon \beta_j^\varepsilon \frac{\partial^2 u^0}{\partial x_i \partial x_j}. \end{aligned}$$

Note that  $\tilde{\beta}_0$  satisfies the same decay estimate (3.12) as  $\beta_0$ , and proceeding along the same line that leads to Lemma 3.6, we obtain

$$\begin{aligned} \int_{\tau_\varepsilon} \left| \nabla \tilde{\beta}_0^\varepsilon \partial_n (u^0 - \pi_h u^0) \right|^2 dx &\leq C \varepsilon^{-2} \int_{\tau_\varepsilon \cap \Gamma_\varepsilon} \left| \nabla (u^0 - \pi_h u^0) \right|^2 dx_1 \int_0^h e^{-2\delta x_2/\varepsilon} dx_2 \\ &\leq C \varepsilon^{-1} \int_{\tau_\varepsilon \cap \Gamma_\varepsilon} \left| \nabla (u^0 - \pi_h u^0)(x_1, x_2) \right|^2 dx_1. \end{aligned}$$

By the trace inequality, we get

$$\begin{aligned} \left\| \nabla \tilde{\beta}_0^\varepsilon \partial_n (u^0 - \pi_h u^0) \right\|_{L^2(\tau_\varepsilon)} &\leq C \varepsilon^{-1/2} \left\| \nabla (u^0 - \pi_h u^0) \right\|_{L^2(\tau_\varepsilon)}^{1/2} \left\| \nabla^2 (u^0 - \pi_h u^0) \right\|_{L^2(\tau_\varepsilon)}^{1/2} \\ &\leq C (h_{\tau_\varepsilon}/\varepsilon)^{1/2} \left\| \nabla^2 u^0 \right\|_{L^2(\tau_\varepsilon)}. \end{aligned}$$

Proceeding along the same line that leads to the above inequality, we obtain

$$\left\| \nabla \beta_i^\varepsilon \partial_{x_i} (u^0 - \pi_h u^0) \right\|_{L^2(\tau_\varepsilon)} \leq C (h_{\tau_\varepsilon}/\varepsilon)^{1/2} \left\| \nabla^2 u^0 \right\|_{L^2(\tau_\varepsilon)}.$$

The remaining terms may be bounded as follows.

$$\left\| \nabla (u^0 - \pi_h u^0) \right\|_{L^2(\tau_\varepsilon)} \leq C h_{\tau_\varepsilon} \left\| \nabla^2 u^0 \right\|_{L^2(\tau_\varepsilon)},$$

and

$$\left\| \tilde{\beta}_0^\varepsilon \partial_n (\nabla u^0) \right\|_{L^2(\tau_\varepsilon)} \leq C \left\| \nabla^2 u^0 \right\|_{L^2(\tau_\varepsilon)}, \quad \left\| \beta_i^\varepsilon \partial_{x_i} (\nabla u^0) \right\|_{L^2(\tau_\varepsilon)} \leq C \left\| \nabla^2 u^0 \right\|_{L^2(\tau_\varepsilon)}.$$

Combining the above estimates, we obtain the desired estimate.  $\square$

For any element  $\tau$  without rough edge,  $\Pi_h u^\varepsilon = \pi_h u^0$ . The decomposition (4.1) is replaced by  $u^\varepsilon - \Pi_h u^\varepsilon = u^\varepsilon - u_1^\varepsilon + u^0 - \pi_h u^0 + \varepsilon u^1$ . Therefore, we need the a priori estimate for  $u^1$  over elements without rough edge. We divide the elements into three groups; the elements with one rough edge belong to  $\mathcal{T}_h^1$ , the elements with one vertex on the rough boundary belong to  $\mathcal{T}_h^2$ , and the remaining elements belong to  $\mathcal{T}_h^3$ .

LEMMA 4.3. *When  $\tau \in \mathcal{T}_h^2$ , then*

$$\sum_{\tau \in \mathcal{T}_h^2} \left\| \nabla u^1 \right\|_{L^2(\tau)}^2 \leq C h^{-1} \left( 1 + \left\| \nabla u^0 \right\|_{L^\infty(\Omega_\varepsilon)}^2 \right) + C \sum_{\tau \in \mathcal{T}_h^2} \left\| \nabla^2 u^0 \right\|_{L^2(\tau)}^2. \quad (4.5)$$

*When  $\tau \in \mathcal{T}_h^3$ , then*

$$\sum_{\tau \in \mathcal{T}_h^3} \left\| \nabla u^1 \right\|_{L^2(\tau)}^2 \leq C \frac{h}{\varepsilon} \left( 1 + \left\| \nabla u^0 \right\|_{W^{1,\infty}(\Omega_\varepsilon)}^2 \right) + C \sum_{\tau \in \mathcal{T}_h^3} \left\| \nabla^2 u^0 \right\|_{L^2(\tau)}^2. \quad (4.6)$$

*Proof.* For an element  $\tau \in \mathcal{T}_h^2$ , we assume that the two sides intersect with  $\Gamma_\varepsilon$  are given explicitly by  $x_1 = \alpha_1 x_2$  and  $x_1 = \alpha_2 x_2$ , with  $|\alpha_i| \leq c_1$  and the bound  $c_1$  depends only on the minimal angle of  $\tau$ . Using (3.12), a direct calculation gives

$$\|\nabla \beta_0^\varepsilon\|_{L^2(\tau)} \leq C\varepsilon^{-1} \left( \int_\tau e^{-2\delta x_2/\varepsilon} dx \right)^{1/2} \leq C\varepsilon^{-1} \left( \int_0^\infty (\alpha_2 - \alpha_1) x_2 e^{-2\delta x_2/\varepsilon} dx_2 \right)^{1/2} \leq C.$$

A direct calculation gives that for  $i = 1, 2$ , there holds

$$\|\nabla(\partial_{x_i} u^0 \beta_i^\varepsilon)\|_{L^2(\tau)} \leq C \left( \|\nabla u^0\|_{L^\infty(\tau)} + \|\nabla^2 u^0\|_{L^2(\tau)} \right).$$

Combining the above estimates and using the fact that the cardinality of  $\mathcal{T}_h^2$  is  $\mathcal{O}(h^{-1})$ , we obtain (4.5).

Using the facts that the triangulation is regular, for the element in  $k$ -th layer, there exists a constant  $c_0$  such that  $c_0 k h \leq \text{dist}(\tau, \Gamma_\varepsilon) \leq c_0(k+1)h$ . By (3.12), a direct calculation gives

$$\begin{aligned} \|\nabla \beta_0^\varepsilon\|_{L^2(\tau)} &\leq C\varepsilon^{-1} \left( \int_\tau e^{-2\delta x_2/\varepsilon} dx \right)^{1/2} \leq C h_\tau^{1/2} \varepsilon^{-1} \left( \int_{c_0 k h}^{c_0(k+1)h} e^{-2\delta x_2/\varepsilon} dx_2 \right)^{1/2} \\ &\leq C(h/\varepsilon)^{1/2} \exp(-c_0 \delta k h / \varepsilon). \end{aligned}$$

Proceeding along the same line that leads to the above estimate, we have for  $i = 1, 2$ ,

$$\|\nabla(\partial_{x_i} u^0 \beta_i^\varepsilon)\|_{L^2(\tau)} \leq C(h_\tau/\varepsilon)^{1/2} \exp(-c_0 \delta k h / \varepsilon) \|\nabla u^0\|_{L^\infty(\tau)} + C \|\nabla^2 u^0\|_{L^2(\tau)}$$

A combination of the above estimates leads to

$$\|\nabla u^1\|_{L^2(\tau)} \leq C \exp(-c_0 \delta k h / \varepsilon) (h_\tau/\varepsilon)^{1/2} \left( 1 + \|\nabla u^0\|_{L^\infty(\tau)} \right) + C \|\nabla^2 u^0\|_{L^2(\tau)}.$$

Summing up all the elements in  $\mathcal{T}_h^3$  leads to (4.6).  $\square$

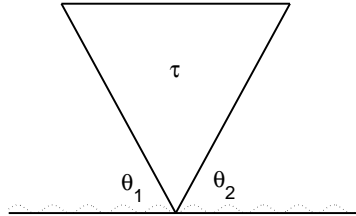


FIG. 4.1. An element with a vertex on the rough boundary.

**4.2. Interpolation error estimate.** The next theorem gives the interpolate error estimate.

THEOREM 4.4. *Let  $u^\varepsilon$  be the solution of the problem (2.1), we have*

$$\begin{aligned} \|\nabla(u^\varepsilon - \Pi u^\varepsilon)\|_{L^2(\Omega_\varepsilon)} &\leq C\varepsilon \left( \|\nabla^2 u^0\|_{H^1(\Omega_0)} + \|\nabla u^0\|_{W^{1,\infty}(\Omega_0)} \right) + Ch \|\nabla^2 u^0\|_{L^2(\Omega_0)} \\ &\quad + C\varepsilon h^{-1/2} (\|\nabla u^0\|_{L^\infty(\Omega_0)} + 1). \end{aligned} \quad (4.7)$$

*Proof.* We start from the following decomposition (4.1). Using Lemma 4.2,

$$\sum_{\tau \in \mathcal{T}_h^1} \|\nabla u_1^\varepsilon - \nabla(\Pi_h u^\varepsilon)_1\|_{L^2(\tau)}^2 \leq C(\varepsilon + h)^2 \sum_{\tau \in \mathcal{T}_h^1} \|\nabla^2 u^0\|_{L^2(\tau)}^2.$$

For  $\tau \in \mathcal{T}_h^2$ , we have  $u_1^\varepsilon - (\Pi_h u^\varepsilon)_1 = u^0 - \pi_h u^0 + \varepsilon u^1$ . Therefore,

$$\sum_{\tau \in \mathcal{T}_h^2} \|\nabla u_1^\varepsilon - \nabla(\Pi_h u^\varepsilon)_1\|_{L^2(\tau)}^2 \leq 2 \sum_{\tau \in \mathcal{T}_h^2} \|\nabla(u^0 - \pi_h u^0)\|_{L^2(\tau)}^2 + 2\varepsilon^2 \sum_{\tau \in \mathcal{T}_h^2} \|\nabla u^1\|_{L^2(\tau)}^2.$$

Using Lemma 4.3, we obtain

$$\sum_{\tau \in \mathcal{T}_h^2} \|\nabla u_1^\varepsilon - \nabla(\Pi_h u^\varepsilon)_1\|_{L^2(\tau)}^2 \leq C(\varepsilon + h)^2 \sum_{\tau \in \mathcal{T}_h^2} \|\nabla^2 u^0\|_{L^2(\tau)}^2 + C \frac{\varepsilon^2}{h} \left( 1 + \|\nabla u^0\|_{L^\infty(\tau)}^2 \right).$$

Proceeding along the same line that leads to the above estimate, we obtain

$$\sum_{\tau \in \mathcal{T}_h^3} \|\nabla u_1^\varepsilon - \nabla(\Pi_h u^\varepsilon)_1\|_{L^2(\tau)}^2 \leq C(\varepsilon + h)^2 \sum_{\tau \in \mathcal{T}_h^3} \|\nabla^2 u^0\|_{L^2(\tau)}^2 + C\varepsilon h \left( 1 + \|\nabla u^0\|_{L^\infty(\Omega_\varepsilon)}^2 \right).$$

Summing up all the above estimates, we obtain

$$\|\nabla u_1^\varepsilon - \nabla(\Pi_h u^\varepsilon)_1\|_{L^2(\Omega_\varepsilon)} \leq C(\varepsilon + h) \|\nabla^2 u^0\|_{L^2(\Omega_\varepsilon)} + C\varepsilon h^{-1/2} \left( 1 + \|\nabla u^0\|_{L^\infty(\Omega_\varepsilon)} \right).$$

By Lemma 4.1,

$$\begin{aligned} \|\nabla \Pi_h u^\varepsilon - \nabla(\Pi_h u^\varepsilon)_1\|_{L^2(\Omega_\varepsilon)}^2 &= \sum_{\tau \in \mathcal{T}_h^1} \|\nabla \Pi_h u^\varepsilon - \nabla(\Pi_h u^\varepsilon)_1\|_{L^2(\tau_\varepsilon)}^2 \\ &\leq C\varepsilon^2 \sum_{\tau \in \mathcal{T}_h^1} \|\nabla u^0\|_{L^\infty(\tau_0)} \leq C \frac{\varepsilon^2}{h} \|\nabla u^0\|_{L^\infty(\Omega_0)}. \end{aligned}$$

Finally, the term  $\|\nabla(u^\varepsilon - u_1^\varepsilon)\|_{L^2(\Omega_\varepsilon)}$  can be bounded by Theorem 3.7. Summing up all the estimates we obtain the desired estimate (4.7).  $\square$

Using the above interpolation estimate, we obtain the main result of this paper.

THEOREM 4.5. *Let  $u^\varepsilon$  and  $u_h$  be the solutions of Problem (2.1) and Problem (2.6), respectively. Then*

$$\begin{aligned} \|\nabla(u^\varepsilon - u_h)\|_{L^2(\Omega_\varepsilon)} &\leq C\varepsilon \left( \|\nabla^2 u^0\|_{H^1(\Omega_0)} + \|\nabla u^0\|_{W^{1,\infty}(\Omega_0)} \right) + Ch \|\nabla^2 u^0\|_{L^2(\Omega_0)} \\ &\quad + C\varepsilon h^{-1/2} (\|\nabla u^0\|_{L^\infty(\Omega_0)} + 1). \end{aligned} \quad (4.8)$$

REMARK 4.6. *We have not estimated the  $L^2$  error of the method, because the  $H^1$  error estimate is not optimal with respect to the regularity of the data. Standard dual argument only yields a suboptimal convergence rate as the original MsFEM [25]. This would be a topic for further study.*

**5. Numerical Examples.** In this section, we perform three numerical experiments to verify the convergence rate and efficiency of the proposed method. We solve Problem (2.1) for different rough domains, different source terms and different boundary fluxes.

**5.1. Implementation.** The implementation of the method is similar to the standard MsFEM [24, 25]. The cell problem (2.3) is numerically solved only for elements with a rough side, and we use  $P_1$  element to solve (2.3) with the subgrid mesh size around  $\varepsilon/20$  in the simulations below.

As an example, we consider a square domain with a rough boundary. The more general case can be done similarly. The domain  $\Omega^\varepsilon$  is given in (3.1) as in Figure 3.1. The function  $\gamma_\varepsilon \simeq \mathcal{O}(\varepsilon)$  that represents the curved boundary will be specified in the examples. We partition  $\Omega_\varepsilon$  with a uniform triangular mesh as in Figure 2.1(b). For a given number  $N$ , we set  $h = 1/N$ . The vertexes far away from the rough boundary are given by  $x_{i,j} = \{(ih, jh)\}$ , where  $i = 0, \dots, N, j = 1, \dots, N$ ; and the vertexes on the rough boundary are given by  $x_{i,0} = (ih, \gamma_\varepsilon(ih))$ ,  $i = 0, \dots, N$ .

The basis function is constructed as follows. For elements without rough boundary, the basis function coincides with the standard linear basis function. For elements with a rough boundary, we compute the multiscale basis function for an element

$$e = \{x \in \mathbb{R}^2 \mid 0 < x_1 < h, \gamma_\varepsilon(x_1) < x_2 < \gamma_\varepsilon(0) + (1 - \gamma_\varepsilon(0)/h)x_1\}$$

for example. Here we actually assume that  $\gamma_\varepsilon(x_1) < \gamma_\varepsilon(0) + (1 - \frac{\gamma_\varepsilon(0)}{h})x_1$  holds for all  $x_1 \in (0, h)$ . In reality, we can always make it true by choosing proper vertexes in the triangulation near the rough boundary. We firstly rescale  $e$  and solve cell problem (2.3) by linear finite element over the rescaled element

$$\hat{e} = \{\hat{x} \in \mathbb{R}^2 \mid 0 < \hat{x}_1 < 1, h^{-1}\gamma_\varepsilon(h\hat{x}_1) < \hat{x}_2 < \gamma_\varepsilon(0)/h + (1 - \gamma_\varepsilon(0)/h)\hat{x}_1\}$$

with a rough boundary  $\hat{\Gamma}_e = \{\hat{x} \in \mathbb{R}^2 \mid 0 < \hat{x}_1 < 1, \hat{x}_2 = h^{-1}\gamma_\varepsilon(h\hat{x}_1)\}$ . We triangulate  $\hat{e}$  by a subgrid with maximum mesh size  $\tilde{h}$ ; see, e.g.,  $\tilde{h} \leq \varepsilon/20$ .  $\hat{\Gamma}_e$  is approximated by  $\hat{\Gamma}_{e,\tilde{h}}$ . For  $g_\varepsilon$  whose average on  $\hat{\Gamma}_{e,\tilde{h}}$  is given by

$$\langle g_\varepsilon \rangle = \int_{\hat{\Gamma}_{e,\tilde{h}}} g_\varepsilon(x_1/h) ds/r \quad \text{with} \quad r = |\hat{\Gamma}_{e,\tilde{h}}|.$$

The flux is given by

$$\hat{\theta}_i(\hat{x}_1) = \begin{cases} b_i/r & \text{if } \|g_\varepsilon - \langle g_\varepsilon \rangle\|_{L^\infty(\hat{\Gamma}_{e,\tilde{h}})} < \varepsilon, \\ b_i \frac{g_\varepsilon}{\langle g_\varepsilon \rangle} & \text{otherwise,} \end{cases}$$

where  $b_1 = 0$ ,  $b_2 = 1$  and  $b_3 = -1$ .

**5.2. Numerical experiments. First Example** In this example, the rough domain is given by

$$\Omega_\varepsilon = \{ x \in \mathbb{R}^2 \mid 0 < x_1 < 1, \varepsilon\gamma(x_1/\varepsilon) < x_2 < 1 \},$$

where  $\gamma(y_1) = (\cos(2\pi y_1) - 1)/10$ . The rough boundary is given by

$$\Gamma_\varepsilon = \{ x \in \mathbb{R}^2 \mid 0 < x_1 < 1, x_2 = \varepsilon\gamma(x_1/\varepsilon) \},$$

and  $\Gamma_D = \partial\Omega_\varepsilon \setminus \Gamma_\varepsilon$ . We choose  $f = 1$  and  $g = 0$  in (2.1), and set homogeneous Dirichlet boundary condition on  $\Gamma_D$  and  $\varepsilon = 1/128$ .

The grid in this example is the uniform triangular grid as the right subfigure in Fig. 2.1 with the mesh size  $h$  varying from  $1/5$  to  $1/160$ . The errors are measured by

$$\text{Err}_{L^2} = \|u_h - \tilde{u}\|_{L^2(\Omega_\varepsilon)}, \quad \text{Err}_{H^1} = \|\nabla u_h - \nabla \tilde{u}\|_{L^2(\Omega_\varepsilon)}.$$

Here  $\tilde{u}$  is a solution computed on an adaptive refined mesh with mesh size  $h \approx 10^{-4}$  by linear finite element.

Fig. 5.1 shows two different scenarios of the convergence behaviour of the method. When the mesh size  $h$  is larger than the roughness parameter  $\varepsilon$ , the method is first order in the  $H^1$  semi-norm and second order in the  $L^2$  norm. When  $h$  is commensurate with  $\varepsilon$ , the method degenerates due to the resonance error. This is consistent with our theoretical prediction, at least for the  $H^1$  error.

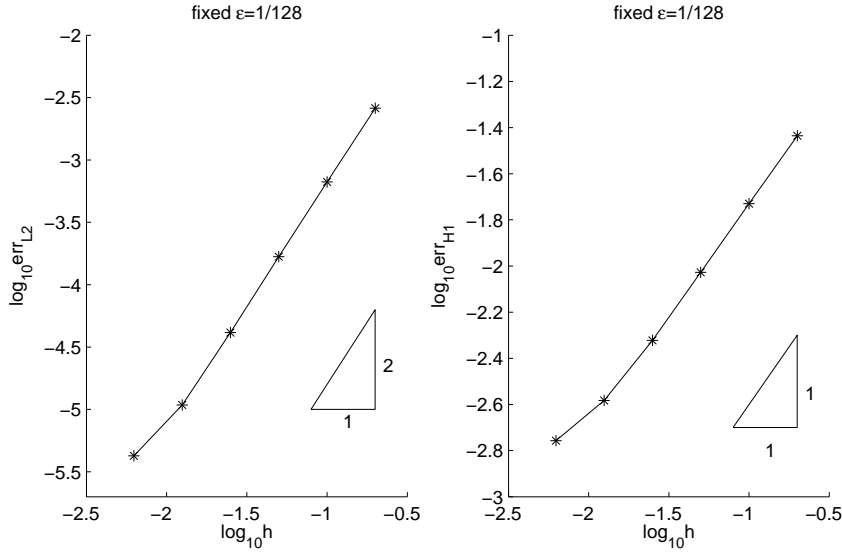


FIG. 5.1. Convergence behavior of the method for the first example.

**Second example** In this example, the domain  $\Omega_\varepsilon$  is the same with that in the first example. Unlike the first example, we choose  $f = 0$  and an inhomogeneous

boundary flux  $g_\varepsilon = (1 - \cos(2\pi x_1/\varepsilon))/2$ . In addition, we impose an inhomogeneous Dirichlet boundary value  $u(x) = (1 - x_2)/2$  on  $\Gamma_D$ .

Uniform triangular grid with the mesh size  $h$  varying from  $1/5$  to  $1/80$  is employed in this example. Fig. 5.2 shows the convergence behavior of the method. It is clear that the method has nearly optimal convergence rate for both the  $H^1$  semi-norm and the  $L^2$  norm when  $h = 1/40 > 2\varepsilon$ , while the resonance error gets to dominate and the convergence rate degenerates when  $h$  is approximately  $1/80$ .

In this example, we use linear finite element to solve the homogenized problem

$$\begin{cases} -\Delta u^0 = 0 & \text{in } \Omega_0, \\ u^0 = \frac{1-x_2}{2} & \text{on } \Gamma_D, \\ \frac{\partial u^0}{\partial n} = \frac{r}{2} & \text{on } \Gamma_0. \end{cases}$$

where  $\Omega_0 = \{x \in \mathbb{R}^2 : 0 < x_1 < 1, 0 < x_2 < 1\}$ ,  $\Gamma_0 = \{(x_1, 0) : 0 < x_1 < 1\}$  and  $r = \int_0^1 [1 + (\gamma'(y_1))^2]^{1/2} dy_1 \approx 1.01$ . This problem is solved by linear finite element with a uniform triangulation of the homogenized domain  $\Omega_0$ . The numerical solutions is denoted by  $u_h^0$ . We compute the following quantities

$$\text{err}_{L^2} = \|u_h^0 - \tilde{u}\|_{L^2(\Omega_0)}, \quad \text{and} \quad \text{err}_{H^1} = \|\nabla u_h^0 - \nabla \tilde{u}\|_{L^2(\Omega_0)},$$

which is reported in Figure 5.2. It seems that the linear finite element method is less accurate as MsFEM. This is due to the fact that the homogenization errors dominate as the mesh is refined. This degeneracy of the convergence rate is more significant for the  $L^2$  error.

**Third Example** In this example, we test the problem with a non-periodic rough boundary, which is not covered by our theoretical results, while the method works as well. The domain is

$$\Omega_\varepsilon = \left\{ x \in \mathbb{R}^2 \mid 0 < x_1 < 1, \frac{\varepsilon}{10}(\gamma(x_1) - 1) < x_2 < 1 \right\}$$

with  $\gamma$  an oscillating function defined as follows. We firstly divide the interval  $(0, 1)$  uniformly as  $0 = s_0 < s_1 < \dots < s_M = 1$  with  $M = 1/\varepsilon = 128$ . The function  $\gamma$  is set to be a piecewise continuous linear function over such partition, with  $\gamma(s_i)$ ,  $i = 0, \dots, M$ , a series of pseudo-random numbers between 0 and 1 generated by a standard C++ library function. The rough boundary

$$\Gamma_\varepsilon = \{ x \in \mathbb{R}^2 \mid 0 < x_1 < 1, x_2 = \varepsilon(\gamma(x_1) - 1)/10 \}.$$

We choose  $f = 1, g = 0$ , and impose a homogeneous Dirichlet boundary condition on  $\Gamma_D$ . We use a uniform triangular grid with the mesh size  $h$  varies from  $1/5$  to  $1/160$ . The results for MsFEM is reported in Fig. 5.3. Similar to the previous examples, we get optimal convergence rate when  $h > 2\varepsilon$ . The resonance errors becomes dominate for the  $L^2$  error when  $h = 1/80$ , but still small for the  $H^1$  error even when  $h = 1/160$ . This might indicate the resonance error for the  $L^2$  error is more pronounced.

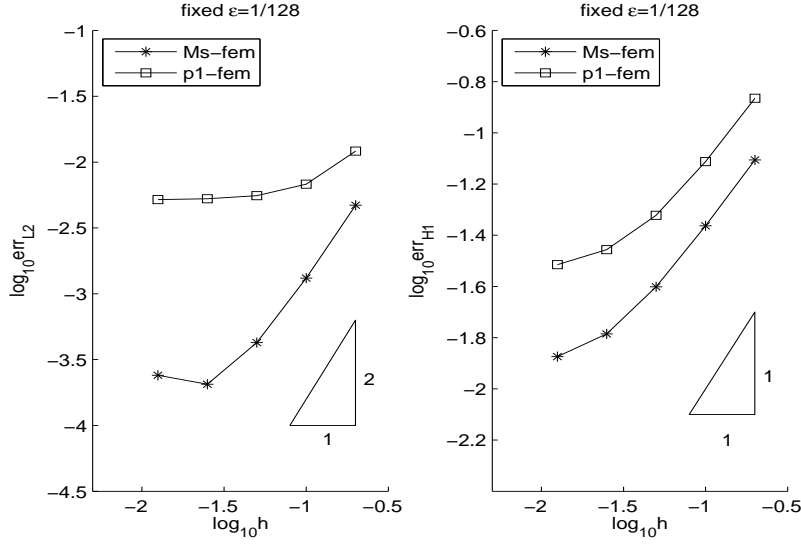


FIG. 5.2. Convergence behavior of the method and standard  $P_1$ -element approximation for the second example.

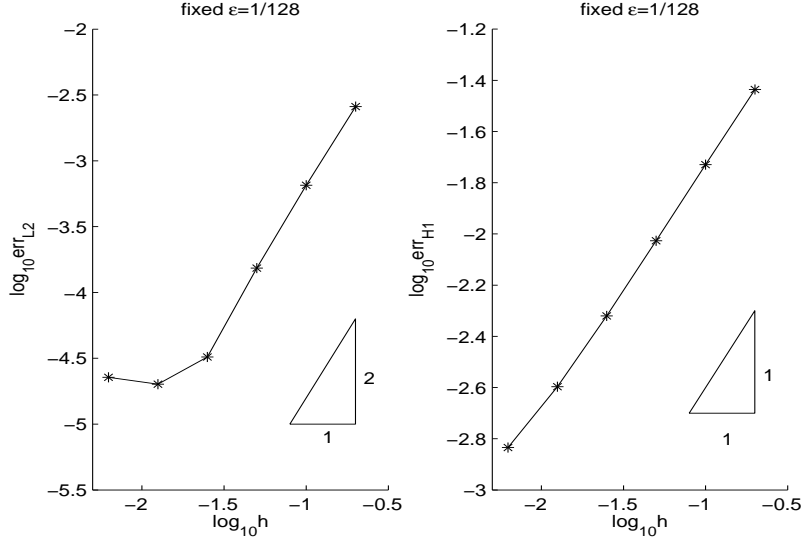


FIG. 5.3. Convergence behavior of the method for the third example.

**Fourth Example** In this example, we test the problem with a discontinuous right-hand side function  $f$  as well as a non-periodic rough boundary, which is slightly more general than that in the previous example. The domain is

$$\Omega_\varepsilon = \{ x \in \mathbb{R}^2 \mid 0 < x_1 < 1, \varepsilon(\gamma(x_1) - 1) < x_2 < 1 \}$$

with  $\gamma$  an oscillating function defined as follows. We firstly divide the interval  $(0, 1)$

by  $0 = s_0 < s_1 < \dots < s_M = 1$  with  $M = 1/\varepsilon = 128$ . In comparison with the third example, here  $s_1, \dots, s_{M-1} \in (0, 1)$  are chosen randomly. For that purpose, we generate a series of pseudo-random numbers between 0 and 1 generated by a standard C++ library function. Then we sort them in a sequence and denoted as  $\{s_i\}$ . The function  $\gamma$  is set to be a piecewise continuous linear function over such partition, with  $\gamma(s_i)$ ,  $i = 0, \dots, M$ , also a series of pseudo-random numbers between 0 and 1. The rough boundary

$$\Gamma_\varepsilon = \{x \in \mathbb{R}^2 \mid 0 < x_1 < 1, x_2 = \varepsilon(\gamma(x_1) - 1)\}.$$

We choose  $g = 0$ , and impose a homogeneous Dirichlet boundary condition on  $\Gamma_D$ . In addition, we choose a discontinuous right hand side function as

$$f(x) = \begin{cases} 1, & \text{if } x_1 < \frac{1}{2}; \\ -1, & \text{if } x_1 \geq \frac{1}{2}. \end{cases}$$

In this case, the homogenized solution  $u_0 \in H^2(\Omega_0)$  and but not in  $H^3(\Omega_0)$ , i.e., it does not satisfy the regularity assumption in our theoretical analysis.

We use a triangular grid with the mesh size  $h$  varies from  $1/5$  to  $1/80$ . The results for MsFEM is reported in Fig. 5.4. Similar to the previous examples, we get optimal convergence rate when  $h > 2\varepsilon$ . We also calculate the 2-norm condition number of the

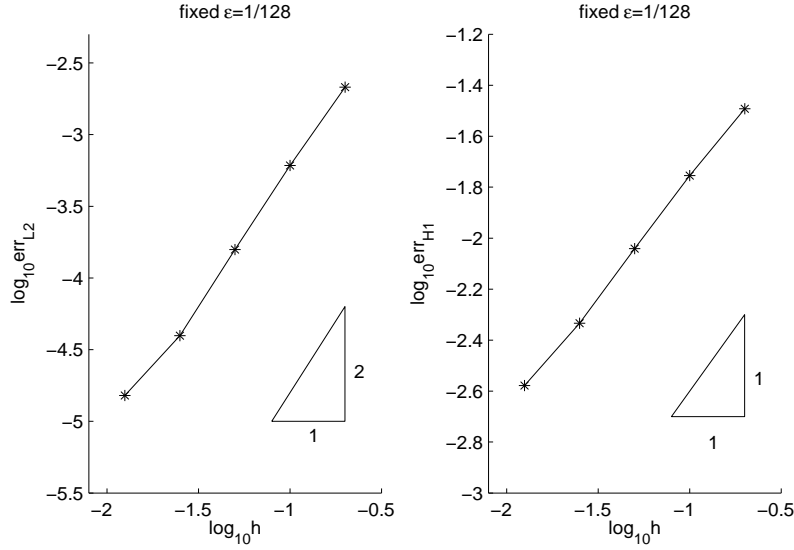


FIG. 5.4. Convergence behavior of the method for the fourth example.

resulting linear system. As shown in Fig. 5.5, the condition number scales as  $\mathcal{O}(h^{-2})$ , which is optimal and is independent of the microstructure.

**Acknowledgement.** We would like to thank the anonymous referees for their many suggestions, that help us to improve the paper.



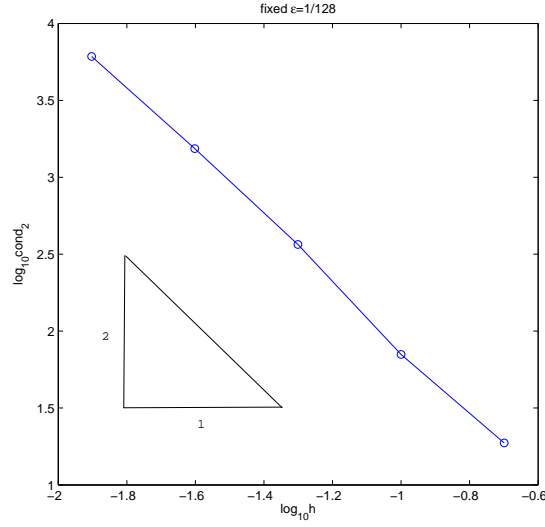


FIG. 5.5. Condition numbers of the MsFEM system.

#### REFERENCES

- [1] A. Abdulle and C. Schwab, *Heterogeneous multiscale FEM for diffusion problems on rough surfaces*, Multiscale Model. & Simul. **3** (2005), 195–220.
- [2] R.A. Adams and J.J.F. Fournier, *Sobolev Spaces*, Academic Press, 2nd ed., 2003.
- [3] G. Allaire and M. Amar, *Boundary layer tails in periodic homogenization*, ESAIM: Control, Opt. Cal. Var. **4** (1999), 209–243.
- [4] Y. Amirat, O. Bodart, U. De Maio, and A. Gaudiello, *Effective boundary condition for stokes flow over a very rough surface*, J. Diff. Eqn. **254** (2013), 3395–3430.
- [5] I. Babuška, G. Caloz, and J. Osborn, *Special finite element methods for a class of second order elliptic problems with rough coefficients*, SIAM J. Numer. Anal. **31** (1994), 945–981.
- [6] I. Babuška, *The finite element method for elliptic equations with discontinuous coefficients*, Computing **5** (1970), 207–213.
- [7] ———, *Homogenization and its applications, mathematical and computational problems*, Numerical Solutions of Partial Differential Equations-III (B. Hubbard, ed.), Academic Press, New York, 1976, pp. 89–116.
- [8] I. Babuška and J.E. Osborn, *Generalized finite element methods: their performance and their relation to mixed method*, SIAM J. Numer. Anal. **20** (1983), 510–536.
- [9] D. Bucur, E. Feireisl, Š. Nečasová, and J. Wolf, *On the asymptotic limit of the navier–stokes system on domains with rough boundaries*, J. Diff. Eqn. **244** (2008), 2890–2908.
- [10] J. Casado-Díaz, M. Luna-Laynez, and F.J. Suárez-Grau, *Asymptotic behavior of the navier–stokes system in a thin domain with navier condition on a slightly rough boundary*, SIAM J. Math. Anal. **45** (2013), 1641–1674.
- [11] P. G. Ciarlet, *The Finite Element Method for Elliptic Problems*, North-Holland, Amsterdam, 1978.
- [12] W. E, *Principles of Multiscale Modeling*, Cambridge University Press, Cambridge, UK, 2011.
- [13] W. E and B. Engquist, *The heterogeneous multiscale methods*, Commun. Math. Sci. **1** (2003), 87–132.
- [14] W. E, P.B. Ming, and P.W. Zhang, *Analysis of the heterogeneous multiscale method for elliptic*

- homogenization problems, *J. Amer. Math. Soc.* **18** (2005), 121–156.
- [15] Y. Efendiev, J. Galvis, and M. Pauletti, *Multiscale finite element methods for flows on rough surfaces*, *Comm. Comput. Phys.* **14** (2013), 979–1000.
  - [16] Y. Efendiev and T.-Y. Hou, *Multiscale finite element methods: theory and applications*, vol. 4, Springer Science & Business Media, 2009.
  - [17] D. Elfverson, E. H. Georgoulis, A. Målqvist, and D. Peterseim, *Convergence of a discontinuous galerkin multiscale method*, *SIAM J. Numer. Anal.* **51** (2013), 3351–3372.
  - [18] D. Elfverson, M. G. Larson, and A. Målqvist, *Multiscale methods for problems with complex geometry*, arXiv:1509.03991v1 (2015).
  - [19] A. Friedman, B. Hu, and Y. Liu, *A boundary value problem for the poisson equation with multi-scale oscillating boundary*, *J. Diff. Eqn.* **137** (1997), 54–93.
  - [20] M. K. Gobbert and C. Ringhofer, *An asymptotic analysis for a model of chemical vapor deposition on a micro structured surface*, *SIAM J. Appl. Math.* **58** (1998), 737–752.
  - [21] W. Hackbusch and S.A. Sauter, *Composite finite elements for the approximation of pdes on domains with complicated micro-structures*, *Numer. Math.* **75** (1997), 447–472.
  - [22] ———, *Composite finite elements for problems containing small geometrical details*, *Comput Visual Sci.* **1** (1999), 15–25.
  - [23] P. Henning and A. Målqvist, *Localized orthogonal decomposition techniques for boundary value problems*, *SIAM J. Sci. Comput.* **36** (2014), 1609–1634.
  - [24] T.-Y. Hou and X.H. Wu, *A multiscale finite element method for elliptic problems in composite materials and porous media*, *J. Comput. Phys.* **134** (1997), 169–189.
  - [25] T.-Y. Hou, X.H. Wu, and Z. Cai, *Convergence of a multiscale finite element method for elliptic problems with rapidly oscillating coefficients*, *Math. Comp.* **68** (1999), 913–943.
  - [26] T.J.R. Hughes, *Multiscale phenomena: Green's functions, the Dirichlet-to-Neumann formulation, subgrid scale models, bubbles and the origins of stabilized methods*, *Comput. Meth. Appl. Mech. Eng.* **127** (1995), 387–401.
  - [27] W. Jager and A. Mikelić, *On the roughness-induced effective boundary conditions for an incompressible viscous flow*, *J. Diff. Eqn.* **170** (2001), 96–122.
  - [28] W. Kohler, G. Papanicolaou, and S. Varadhan, *Boundary and interface problems in regions with very rough boundaries*, *Multiple Scattering and Waves in Random Media* (P.L. Chow, W.E. Kohler, and G. Papanicalou, eds.), North-Holland Publishing Company, 1981, pp. 165–197.
  - [29] A. L. Madureira and F. Valentin, *Asymptotics of the poisson problem in domains with curved rough boundaries*, *SIAM J. Math. Anal.* **38** (2007), 1450–1473.
  - [30] A.L. Madureira, *A multiscale finite element method for partial differential equations posed in domains with rough boundaries*, *Math. Comp.* **78** (2008), 25–34.
  - [31] A. Målqvist, *Multiscale methods for elliptic problems*, *Multiscale Model. Simul.* **9** (2011), 1064–1086.
  - [32] A. Målqvist and D. Peterseim, *Localization of elliptic multiscale problems*, *Math. Comp.* **83** (2014), 2583–2603.
  - [33] ———, *Computation of eigenvalues by numerical upscaling*, *Numer. Math.* **130** (2015), 337–361.
  - [34] W. McLean, *Strongly Elliptic Systems and Boundary Integral Equations*, Cambridge University Press, Cambridge, UK, 2000.
  - [35] A. Mikelić, *Rough boundaries and wall laws*, *Qualitative Properties of Solutions to Partial Differential Equations* (E. Feireisl, P. Kaplicky, and J. Malek, eds.), Lecture notes of Necas Center for mathematical modeling, Matfyzpress, Publishing House of the Faculty of Mathematics and Physics Charles University in Prague, Prague, 2009, pp. 103–134.
  - [36] N. Neuss, M. Neuss-Radu, and A. Mikelić, *Effective laws for the poisson equation on domains with curved oscillating boundaries*, *Applicable Anal.* **85** (2006), 479–502.
  - [37] J. Nevard and J.B. Keller, *Homogenization of rough boundaries and interfaces*, *SIAM J. Appl. Math.* **57** (1997), 1660–1686.
  - [38] S. Nicaise and S.A. Sauter, *Efficient numerical solution of Neumann problems on complicated*

- domains*, *Calcolo* **43** (2006), 95–120.
- [39] O.A. Oleinik, A.S. Shamayev, and G.A. Yosifian, *Mathematical Problems in Elasticity and Homogenization*, North-Holland, Amsterdam, 1992.
  - [40] H. Owhadi and L. Zhang, *Metric based up-scaling*, *Comm. Pure Appl. Math.* **60** (2007), 675–723.
  - [41] D. Peterseim and S. Sauter, *Finite element methods for the stokes problem on complicated domains*, *Comput. Meth. Appl. Mech. Engrg* **200** (2011), 2611–2623.
  - [42] M. Rech, S. Sauter, and A. Smolianski, *Two-scale composite finite element method for dirichlet problems on complicated domains*, *Numer. Math.* **102** (2006), 681–708.
  - [43] R. Verfürth, *A review of a posteriori error estimation and adaptive mesh-refinement techniques*, Wiley, 1996.
  - [44] X. Xu and X. P. Wang, *Derivation of the wenzel and cassie equations from a phase field model for two phase flow on rough surface*, *SIAM J. Appl. Math* **70** (2010), 2929–2941.